manufacturer's instructions. Hybridization was performed in Ultra Hyb solution (Ambion, Austin, TX) at 42°C overnight for Hath1 and at 55°C for 2 hours for β-actin. Visualization of the hybridized signals was conducted with the BAS-2000 image analyzing system (Fuji Film, Tokyo, Japan).

Reporter Assays

SW480 cells were transiently transfected with 10 ng of renilla luciferase reporter plasmid pRL-TK-Luc (Promega) along with 100 ng of either TOPflash, FOPflash, or an E-box-Luc reporter plasmid. One microgram of the expression plasmid pCMV-Flag-WT-Hath1 or its empty control, and the same amount of pCS2-APC2 or its empty control, were also cotransfected, keeping the total amount of plasmid per transfection constant. Transfections of 293T cells were performed identically, except for substituting the pCS2-APC2 with the pRL5-Wnt1 and the pCS2 vector with the pRL5 vector, respectively. After 12 hours of transfection, cells were cultured for 24 hours and lysed by 3 cycles of freezing and thawing. Firefly luciferase activity was normalized with renilla luciferase activity in each sample by using the Dual Luciferase Kit (Promega). The E-box-dependent luciferase activities were shown as arbitrary units normalized by renilla luciferase activity, and the β-catenin/TCF-dependent luciferase activities were shown as a ratio of TOPflash and FOPflash.

Immunocytochemistry

SW480 cells were cotransfected on a sterile glass coverslip with 1 μg of a bicistronic expression vector pMX-Flag-Hath1-IRES-GFP or its empty control together with 1 μg of a pCS2-APC2 or pCS2 vector as indicated. Twelve hours after transfection, cells were fixed with 4.0% paraformaldehyde, rinsed twice with PBS, and permeabilized with 0.2% Triton X-100 in PBS, followed by incubation for 1 hour in 3% bovine serum albumin-containing PBS to block nonspecific antibody binding. The samples were incubated for 3 hours at 37°C with either mouse anti-Flag antibody (1 μg/mL) or mouse anti-MUC2 antibody (1 μg/mL, Ccp58; Santa Cruz Biotechnology), washed twice with PBS, and then incubated for 1 hour at 37°C with Alexa 594-conjugated anti-mouse fluorescent secondary antibodies (Molecular Probes, Eugene, OR). The cells were also counterstained with 4′,6-diamidino-2-phenylindole (Vector Laboratories, Burlingame, CA) to visualize nuclei. The samples were washed 3 times with PBS and analyzed with an epifluorescence microscope (BX-50; Olympus, Tokyo, Japan) equipped with a PDMC device camera (Polaroid, Waltham, MA) for coexistence of the fluorescent signals of the secondary antibodies (Flag-Hath1 or MUC2 protein) and green fluorescent protein, the latter of which is translated from the IRES element fused downstream of the coding region for Flag-Hath1 protein. Images were processed in Adobe Photoshop software (Adobe Systems Inc, San Jose, CA).

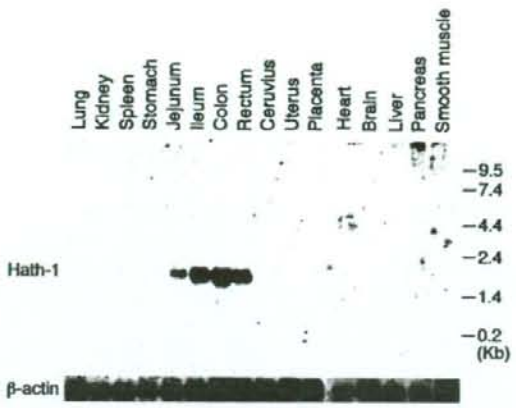

Figure 1. Expression of Hath1 mRNA is confined to the lower gastrointestinal tract. Hath1 mRNA expression in various adult human tissues was analyzed by Northern blotting by using a complementary DNA probe corresponding to nucleotides +1/+749 of the *Hath1* gene. Hybridization with a probe for β-actin is shown as a loading control. Hath1 mRNA is indeed exclusively expressed in the gastrointestinal tract of the human adult body. Moreover, the amount of Hath1 mRNA expression within the gastrointestinal tract increases as it reaches downward to the anal verge, where the population of secretory lineage epithelial cells is also increased.

Immunohistochemistry

Normal and cancerous colonic mucosae were obtained from 4 patients with colorectal cancer who underwent colectomy. Written informed consent was obtained from all patients, and these experiments were approved by the Tokyo Medical and Dental University Hospital Ethics Committee on Human Subjects. Immunohistochemistry for β-catenin was performed as described elsewhere,[25] using anti-β-catenin antibody (BD Transduction, San Diego, CA) and the standard ABC method (Vectastain; Vector Laboratories). Staining was developed by addition of diaminobenzidine (Vector Laboratories). Hath-1 antibody was generated by immunizing rabbits with Hath-1 peptide (247–265). Samples were fixed with 4% paraformaldehyde and subjected for staining using a TSA Signal Amplifying Kit (Molecular Probes) following the manufacturer's instructions. Staining was developed by addition of Alexa 488-conjugated tyramide. Sections were also counterstained with 4′,6-diamidino-2-phenylindole (Vector Laboratories) to visualize nuclei. Stained samples were analyzed with an epifluorescence microscope (BX-50; Olympus) equipped with a PDMC device camera (Polaroid).

Results

Expression of Hath1 mRNA Is Confined to the Lower Gastrointestinal Tract

The mRNA expression of Math1 and Hath1 is reported to be confined to the gastrointestinal tract in adult mice[26] and humans,[19] respectively. However, precise analysis of the expression of Hath1 mRNA within the gastrointestinal tract has never been reported. Thus, we compared mRNA expression of Hath1 in each section of the adult human gastrointestinal tract by Northern blotting. Results revealed that Hath1 mRNA is indeed exclusively expressed in the gastrointestinal tract, from the jejunum to the rectum (Figure 1). Moreover, the amount of Hath1 mRNA expression was significantly increased in the colon, compared with the jejunum or the ileum, where the population of secretory lineage epithelial cells is relatively increased. These results suggested that Hath1 expression is strictly regulated by mRNA expression, at least in the normal adult human body, and may have critical roles especially in the differentiation of colonocytes into secretory lineage cells.

Hath1 Undergoes Proteasome-Mediated Proteolysis in Human Colon Cancer–Derived Cells

To further analyze the functional role of Hath1 in colonocyte differentiation, we first asked whether an overexpression of Hath1 could change any phenotype of human colon-derived epithelial cells. Because the results of the former section suggested that expression of Hath1 mRNA may directly lead to Hath1 protein

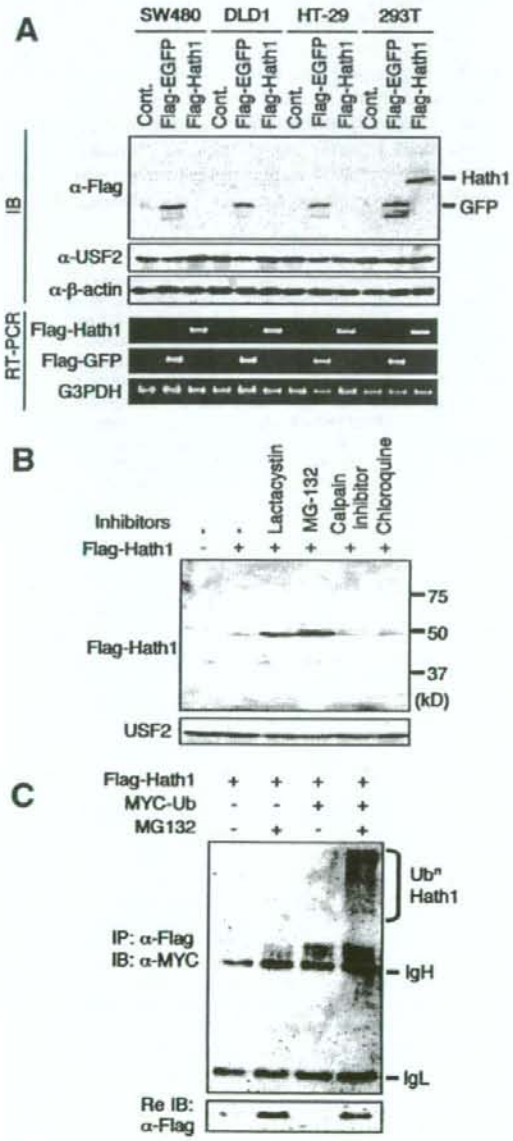

Figure 2. Hath1 undergoes proteasome-mediated proteolysis in human colon cancer–derived cells. (*A*) Hath1 protein expression cannot be detected after introduction of a gene encoding Hath1 in human colon cancer–derived cells. An expression plasmid encoding either Flag-tagged WT-Hath1 (Flag-Hath1), Flag-tagged EGFP (Flag-EGFP), or an empty control (Cont.) was transfected into human colon cancer–derived cell lines (SW480, DLD-1, and HT-29) or a noncolonic cell line (293T). Introduction of the genes was confirmed by semiquantitative RT-PCR, and the expression of the corresponding protein was examined by immunoblot (IB). While Flag-tagged EGFP shows stable expression of both mRNA and protein in every cell line, protein expression of Flag-Hath1 is detectable in 293T cells but not in colon cancer cell lines. Semiquantitative RT-PCR shows an equal amount of Flag-Hath1 mRNA expression in both 293T cells and colon cancer cell lines. (*B*) Hath1 protein is degradated by a proteasome-mediated mechanism in colon cancer cells. Flag-WT-Hath1 (Flag-Hath1) expression vector was transfected into SW480 cells and treated with various inhibitors of cellular proteolytic systems during protein expression. Expression of FLAG-Hath1 protein was examined by immunoblot using anti-Flag antibodies. Only the inhibitors of the proteasome pathway (lactacystin and MG132), but not any other inhibitor of the proteolytic pathway (calpain inhibitor and chloroquine), significantly increased protein expression of FLAG-Hath1. (*C*) Hath1 protein is polyubiquitinated in colon cancer cells. Expression vectors for Flag-Hath1 and Myc-tagged ubiquitin (Myc-Ub) were cotransfected into SW480 cells. Following transfection, cells were treated with or without MG132 during protein expression. The lysates were immunoprecipitated (IP) with anti-Flag antibodies and subjected to immunoblot (IB) using anti-Myc antibodies. Cotransfection of Flag-Hath1 and Myc-Ub, followed by inhibition of the proteasome pathway by MG132, allowed detection of the stabilized, polyubiquitinated FLAG-Hath1 protein by anti-myc antibody. Two bands labeled as IgH and IgL represent heavy chain and light chain of anti-Flag antibody used for immunoprecipitation, respectively. Reprobing the same membrane (Re IB) with anti-FLAG antibody shows efficient immunoprecipitation of FLAG-Hath1 protein only in MG132-treated conditions, because FLAG-Hath1 proteins are readily ubiquitinated and degradated in other conditions.

expression and function to regulate differentiation in colonocytes, we introduced an expression plasmid vector encoding Flag-tagged Hath1 (Flag-WT-Hath1) into various human colon cancer–derived epithelial cell lines. Surprisingly, significant expression of FLAG-Hath1 protein could not be observed in all 3 colon cancer cell lines examined, which were SW480, DLD1, and HT-29. This was not due to low efficiency of transfection or poor sensitivity of the immunoblot, because expression of Flag-EGFP protein could be easily detected by introducing the same amount of the expression plasmid having the same plasmid backbone (Figure 2*A*). Furthermore, semiquantitative RT-PCR showed an equal amount of Flag-Hath1 or Flag-EGFP mRNA expression in every colon cancer cell line, confirming the efficient transfection of the FLAG-Hath1 gene. However, Flag-Hath1 and Flag-EGFP showed equal expression of both mRNA and protein in 293T cells. These results suggested that there might be a posttranscriptional regulation of Hath1 expression involving protein degradation, specifically in colon cancer cells (Figure 2*A*). To confirm the involvement of proteolysis in the significantly decreased expression of Hath1 protein in colon cancer cell lines, we used various pharmacologic inhibitors of the cellular proteolytic system. When SW480 cells were treated with these inhibitors after transfection of Flag-Hath1 expression vectors, inhibitors such as calpain inhibitor or chloroquine had no effect on protein expression of Flag-Hath1 (Figure 2*B*). In sharp contrast, treatment with proteasome inhibitors such as MG132 or lactacystin significantly increased the protein expression of Flag-Hath1, suggesting that Hath1 protein is degradated by the proteasome-mediated proteolysis in colon cancer cells (Figure 2*B*). Because proteasome-mediated proteolysis often requires conjugation of ubiquitins to the target protein,[27,28] we next examined whether Hath1 proteins are ubiquitinated before degradation in

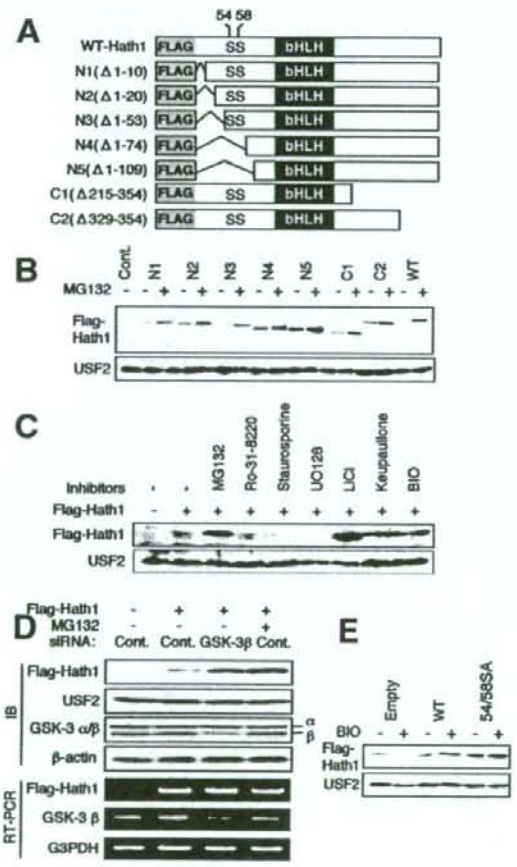

Figure 3. GSK3β-mediated Hath1 proteolysis in colon cancer cells critically requires S54 and S58 of Hath1 protein. (*A*) Schematic representation of various FLAG-tagged Hath1 mutants. Deletion mutants of the N-terminal or C-terminal part of the Hath1 protein are designated as N1–N4 or C1 and C2 mutants. The deleted region of each mutant is designated by amino acid numbers, that is, Δ1–10 designates deletion of amino acid 1–10 of Hath1 protein. The basic helix-loop-helix domain located in the central region as well as 2 serine (S) residues at positions 54 (S54) and 58 (S58) are shown. (*B*) The region consisting of amino acids 54–74 is required for active degradation of Hath1 protein. The wild-type and mutant Hath1 protein shown in *A* were expressed with or without MG132 treatment in SW480 cells. Protein expression was detected by immunoblot using anti-FLAG antibody. N4 and N5 mutant, but not any other wild-type or mutant Hath1 protein, showed no difference in the amount of protein expression between MG132-treated or untreated conditions. (*C*) Proteolysis of Hath1 is suppressed by specific inhibitors of GSK3β in colon cancer cells. Flag-WT-Hath1 was transfected into SW480 cells and treated with various protein kinase inhibitors. Protein expression was detected by immunoblot using anti-FLAG antibody. FLAG-Hath1 protein is stabilized by the proteasome inhibitor (MG132) and kinase inhibitors specific for GSK3β (LiCl, kenpaullone, BIO) but not by other kinase inhibitors (Ro-31-8220, staurosporine, UO126). (*D*) Gene silencing of GSK3β by siRNA increases Hath1 protein expression. An siRNA specific for GSK3β was cotransfected with Flag-WT-Hath1 into SW480 cells. Transfection of a nonsense siRNA served as a control (Cont.). Expression of FLAG-Hath1 and GSK3β was analyzed by semiquantitative RT-PCR and immunoblotting. Transfection of a GSK3β-specific siRNA significantly reduced both mRNA and protein expression of GSK3β. The specific knockdown of GSK3β increased protein expression of cotransfected FLAG-Hath1, which could also be induced up to a similar level by MG132 treatment. (*E*) S54 and S58 are the critical residues for GSK3β-mediated Hath1 proteolysis. An empty vector encoding no protein (*Empty*), or FLAG-tagged, wild-type (WT), or 54/58 SA mutant of Hath1 (54/58SA), in which both S54 and S58 of the Hath1 protein were substituted to alanines, was transfected into SW480 cells. The effect of treatment with a GSK3β-specific inhibitor (BIO) on the expression of each protein in SW480 cells was examined by immunoblot. 54/58 SA mutant of Hath1, but not the WT, showed stable protein expression without BIO treatment. A trace signal examined in the left end of the "Flag-Hath1" blot has been determined to be a nonspecific signal and does not represent expression of a Flag-tagged protein.

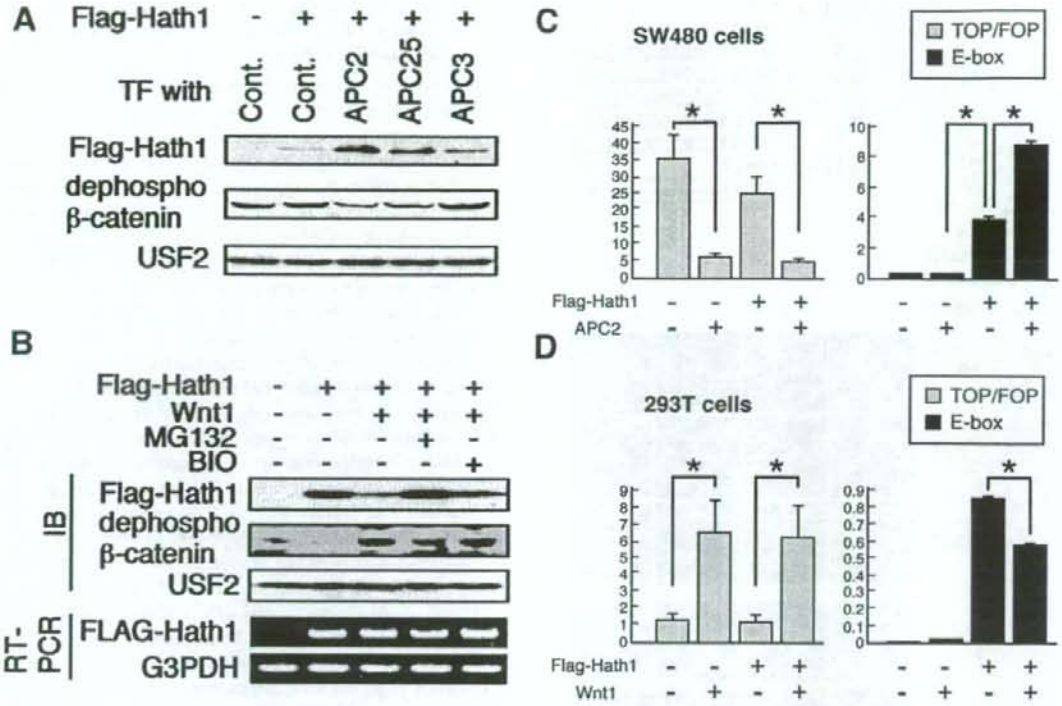

Figure 4. The canonical Wnt pathway reciprocally regulates Hath1 and β-catenin protein stability and downstream transcription activities via GSK3β. (*A*) Suppression of Wnt signaling in colon cancer cells increases expression of Hath1 protein. Flag-WT-Hath1 and APC mutants that are capable (APC2 and APC25) or incapable (APC3) of destabilizing β-catenin were cotransfected into SW480 cells. Cell lysates were subjected to immunoblotting for Flag-Hath1 (anti-Flag) or dephosphorylated β-catenin. Cotransfection of APC2 or APC25, but not of APC3, reduced the amount of dephosphorylated β-catenin protein and conversely increased the amount of Hath1 protein. (*B*) Activation of Wnt signaling induces degradation of Hath1 protein. Expression vectors for Flag-Hath1 and Wnt1 were cotransfected into 293T cells. Cells were cultured with or without MG132 or BIO, and protein expression of Hath1 and dephosphorylated β-catenin was analyzed by immunoblotting (IB). Equivalent transfection of Flag-Hath1 was confirmed by semiquantitative RT-PCR. Expression of Wnt1 in 293T cells induced dephosphorylation of β-catenin protein and also reduced expression of the cotransfected Flag-Hath1 protein (*lane 3*). This reduction of Flag-Hath1 protein is rescued by addition of a proteasome inhibitor (MG132) or a specific inhibitor of GSK3 (BIO). (*C*) Suppression of Wnt signaling in colon cancer cells up-regulates Hath1-mediated, E-box–dependent transcription and reciprocally down-regulates β-catenin/TCF–dependent transcription. Flag-WT-Hath, APC2, and designated reporter constructs were cotransfected into SW480 cells. E-box–dependent luciferase activities were shown as arbitrary units after normalization by renilla luciferase activity, and β-catenin/TCF–dependent luciferase activities are shown as a ratio of TOPflash and FOPflash. *$P < .005$. Transfection of APC2 significantly down-regulated β-catenin/TCF–dependent transcription but conversely up-regulated Hath1-mediated, E-box–dependent transcription in SW480 cells. (*D*) Activation of Wnt signaling in 293T cells down-regulates Hath1-mediated, E-box–dependent transcription and reciprocally up-regulates β-catenin/TCF–dependent transcription. Flag-WT-Hath, Wnt1, and designated reporter constructs were cotransfected into 293T cells. E-box– and β-catenin/TCF–dependent transcriptional activities were measured as described in the former section. *$P < .005$. Transfection of Wnt1 significantly up-regulated β-catenin/TCF–dependent transcription but conversely down-regulated Hath1-mediated, E-box–dependent transcription in 293T cells.

SW480 cells. For this purpose, Myc-tagged ubiquitin and Flag-Hath1 were coexpressed in SW480 cells and, subsequently, proteasome-mediated degradation was inhibited by MG132. When the cell lysates were immunoprecipitated by anti-Flag antibody, conjugation of Myc-tagged ubiquitin to Flag-Hath1 protein was detectable by immunoblot using anti-Myc antibody (Figure 2*C*). Ubiquitinated Hath1 protein appeared as a broad band on the membrane, suggesting that it is conjugated with random numbers of multiple ubiquitins (polyubiquitinated). Reprobing the same membrane (Re IB) with anti-FLAG antibody showed efficient immunoprecipitation of FLAG-Hath1 protein only in MG132-treated conditions, because FLAG-Hath1 proteins are readily ubiquitinated and degradated in other conditions (Figure 2*C*). These results collectively suggested that Hath1 proteins are polyubiquitinated before degradation by the proteasome-mediated proteolysis in colon cancer cells.

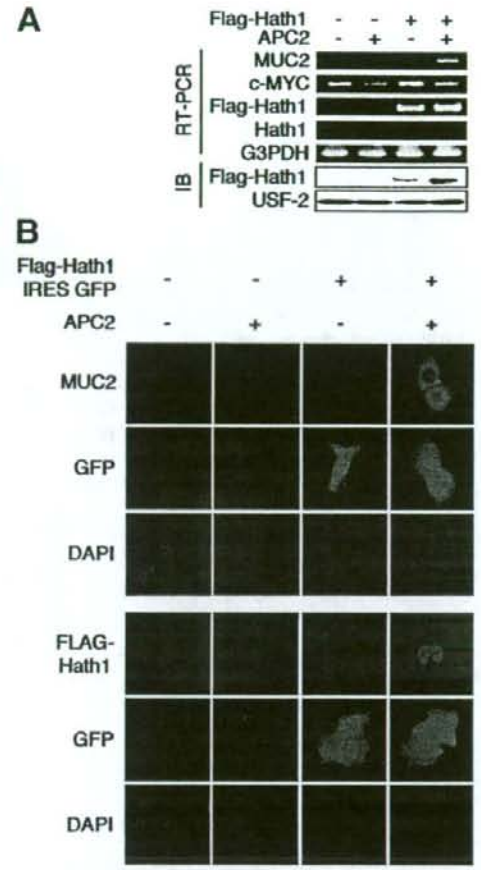

Figure 5. Inactivation of canonical Wnt signaling is required for Hath1-mediated colonocyte differentiation. (*A*) Suppression of canonical Wnt signaling in colon cancer cells is required for Hath1-mediated colonocyte differentiation. Expression plasmids for Flag-Hath1 and APC2 were cotransfected into SW480 cells. Expression of MUC2, C-MYC, Flag-Hath1, endogenous Hath1 (Hath1), and G3PDH mRNA was analyzed by RT-PCR. In the same experiment, protein expression of Flag-Hath1 and USF2 was examined by immunoblotting (IB). The expression of the goblet cell–specific gene *MUC2* was induced only when both FLAG-Hath1 and APC2 were expressed in SW480 cells. (*B*) MUC2 protein is expressed in cells that Hath1 protein stabilized by suppression of Wnt signaling. A bicistronic expression vector pMX-Flag-Hath1-IRES-GFP or its empty control was cotransfected with an expression vector for APC2 into SW480 cells. Cells were stained by fluorescent immunocytochemistry for MUC2 (*upper half, red*) or Flag-Hath1 (*lower half, red*). The green signal of green fluorescent protein (GFP) represents transcription of Flag-Hath1, encoded upstream of GFP and the IRES element. Expression of MUC2 protein is induced only when FLAG-Hath1 protein is stabilized by cotransfecting FLAG-Hath1 and APC2 into SW480 cells. DAPI, 4′,6-diamidino-2-phenylindole.

GSK3β-Mediated Hath1 Proteolysis in Colon Cancer Cells Critically Requires S54 and S58 of Hath1 Protein

Former results confirmed that Hath1 protein is constitutively degradated by proteasome-mediated proteolysis in colon cancer cells. This raised the question whether there is a specific region within the Hath1 protein that is critically required for the present proteolysis system. Although it is well known that Hath1 protein contains a basic helix-loop-helix domain that is critically required for binding to the target sequence of DNA,[26,29] other regions of the protein have not been functionally characterized. To determine the region that may be critically required for the degradation of Hath1 protein, various mutants of Flag-tagged Hath1 protein (Figure 3*A*) were expressed in SW480 cells (Figure 3*B*). Immunoblot using anti-Flag antibody revealed that, although a trace amount of Flag-tagged protein was detected without MG132 treatment by increasing the amount of loaded lysates, deleting up to 53 amino acids of the N-terminal end (N1 to N3), or 140 amino acids of the C-terminal end (C1 and C2), appeared to have no effect on protein stability of the Hath1 protein. However, deletions up to 74 or 109 amino acids of the N-terminal end (N4 and N5) showed markedly stable expression of Hath1 protein without MG132 treatment. These results indicated that the region between amino acids 54 and 74 is critically required for proteasome-mediated Hath1 proteolysis.

The region between amino acids 54 and 74 of the Hath1 protein included 2 serine and 3 threonine residues. It is well known that one of the important mechanisms required for proteasome-dependent degradation is the phosphorylation of specific amino acid residues.[30,31] Based on these data, we searched, using Scansite software (Scansite, Boston, MA), for whether a putative phosphorylation site may exist within the region between amino acids 54 and 74 of the Hath1 protein. Surprisingly, a distinct site extending from serine residue at position 54 (S54) to position 58 (S58) matched the consensus substrate sequence (S/T-X-X-X-S/T) for GSK3β (Figure 3*A*). These results raised a possibility that Hath1 protein is a substrate of GSK3β, and therefore Hath1 protein degradation is regulated by the phosphorylation of specific serine residues by GSK3β. To determine whether kinase activity of GSK3β is required for Hath1 protein degradation, SW480 cells were treated with inhibitors of various protein kinases and examined for FLAG-Hath1 protein expression by immunoblot (Figure 3*C*). Confirming the in silico search for putative phosphorylation sites, FLAG-Hath1 protein was stabilized by the proteasome inhibitor, MG132, and kinase inhibitors specific for GSK3β such as LiCl, kenpaullone, and BIO, but not by other kinase inhibitors such as Ro-31-8220, staurosporine, or UO126, which does not inhibit GSK3β.

To further confirm the involvement of GSK3β in Hath1 proteolysis, we used an siRNA-mediated gene knockdown system to specifically knock down GSK3β gene expression in colon cancer cells. Transfection of GSK3β-specific siRNA into SW480 cells successfully decreased both mRNA and protein expression of GSK3β in SW480 cells (Figure 3*D*). Under this condition, expression of the cotransfected Flag-Hath1 protein was significantly increased up to a comparable level with MG132 treatment. No change was observed in the quantity of Flag-Hath1 mRNA, suggesting that the increase of Flag-Hath1 protein is due to increased protein stability. These results further confirmed that kinase activity of GSK3β is critically required for Hath1 protein degradation in colon cancer cells.

We next examined whether the 2 serine residues found in the putative GSK3β target region (S54 and S58) are critically required for GSK3β-mediated Hath1 proteolysis. For this purpose, a mutant Flag-Hath1 in which 2 serine residues (S54 and S58) were replaced into 2 alanines (54/58SA) was expressed in SW480 cells. Consistently, examination of protein expression by immunoblot revealed that the 54/58 SA mutant of Hath1 (54/58SA), but not the wild type, showed stable protein expression without inhibition of GSK3β by BIO treatment.

These data collectively indicated that the kinase activity of GSK3β is critically required for the degradation of Hath1 in colon cancer cells and also that the 54th and 58th serine residues of the Hath1 protein are critically required for GSK3β-mediated Hath1 proteolysis.

The Canonical Wnt Pathway Reciprocally Regulates Hath1 and β-catenin Protein Stability and Downstream Transcription Activities via GSK3β

Former findings raised an important question as to how the kinase function of GSK3β for Hath1 proteolysis is regulated by the upstream signaling events in colon cancer cells. GSK3β is known to participate not only in the canonical Wnt pathway but also in other pathways such as insulin signaling.[32] However, it is also known that the kinase activity of GSK3β is regulated by a single signaling pathway within a single cell and is usually not modified or affected by multiple pathways.[33] In most human colorectal cancer cells, Wnt signal is aberrantly activated by various gene mutations. Indeed, all the colon cancer cell lines used in this study harbor mutations in the *APC* gene, which suppress the kinase activity of GSK3β on β-catenin phosphorylation and consequently stabilize β-catenin protein.[18] Moreover, a recent study showed that the Wnt signal activates GSK3 to phosphorylate LRP6 in opposite relationship to β-catenin.[34] Therefore, we hypothesized that GSK3β kinase activity is dominantly regulated by Wnt signaling in colon cancer cells, and the aberrant activation of this signal may be involved in Hath1 protein degradation via GSK3β. To confirm the hypothesis, we first examined whether Hath1 protein may be stabilized by the inactivation of the aberrant Wnt signaling in colon cancer cells. For this purpose, we used SW480 cells, in which aberrant Wnt signaling is caused by truncated mutation of *APC*. When the aberrant Wnt signaling of SW480 cells was

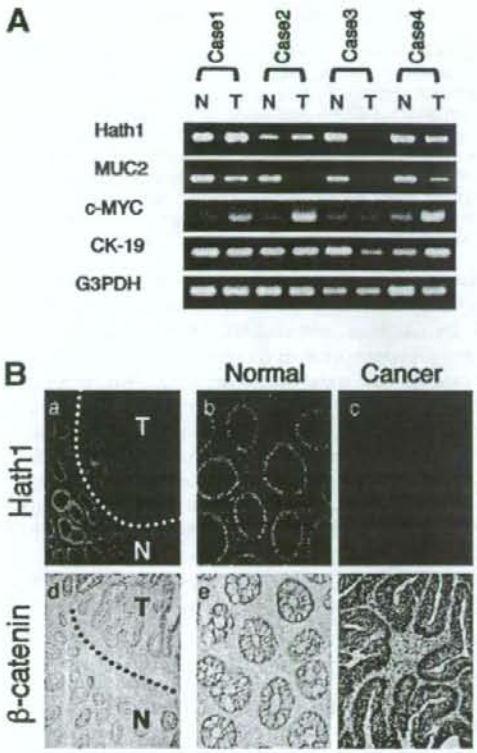

Figure 6. Hath1 protein expression is decreased in human colon cancer tissues expressing Hath1 mRNA and nuclear-located β-catenin protein. (*A*) Hath1 mRNA is expressed in both normal and cancer tissues of human colon. Four cases of colorectal cancer were examined (cases 1–4). N, normal colon mucosa; T, colon cancer tissue of each patient. Semiquantitative analysis of Hath1, C-MYC, MUC2, CK-19, and G3PDH mRNA expression was performed by RT-PCR. CK-19 served as a control for epithelial cell population, whereas G3PDH served as a loading control. In cases 1, 2, and 4, Hath1 mRNA is expressed in both normal and cancer tissue. (*B*) Hath1 protein expression is decreased in colon cancer tissue. The border lesion of the tumor in case 2 was subjected to immunohistochemical analysis. A lower magnification of the border lesion of the tumor (*a* and *d*) and also the magnified view of the cancer tissue (*c* and *f*) and the adjacent normal mucosa (*b* and *e*) are presented. Tissue sections were stained with either anti-Hath1 (Alexa 488, green signal, *a–c*) or anti–β-catenin (diaminobenzidine, brown signal, *d–f*). The figures show a significant decrease of Hath1 staining in cancer tissues compared with normal colonic mucosa, whereas nuclear located β-catenin is significantly increased in cancer tissues (original magnification: *a* and *d*, 100×; *b*, *c*, *e*, and *f*, 400×).

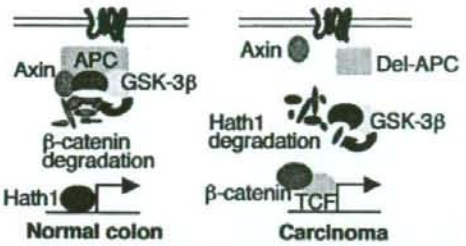

Figure 7. Schematic representation of Wnt-GSK3β–mediated regulation of colonocyte differentiation and proliferation. In normal colonocytes, differentiation is accelerated by turning off the Wnt signaling, which leads to GSK3β-mediated degradation of β-catenin protein and up-regulation of Hath1-mediated transcription of yet-unknown target genes. Conversely, during transformation of colonocytes into carcinoma cells, proliferation is accelerated by constitutive activation of Wnt signaling, which leads to GSK3β-mediated degradation of Hath1 protein and up-regulation of β-catenin/TCF–mediated transcription.

inactivated by transfecting APC mutants (APC2 and APC25) that are capable of forming complexes with β-catenin, Axin, and GSK3β,[22] the amount of endogenous dephosphorylated β-catenin as a stabilized form of β-catenin was significantly decreased but, surprisingly, the expression of cotransfected Flag-WT-Hath1 protein was significantly increased (Figure 4*A*). Transfection of the C-terminal fragment of human APC (APC3; amino acids 2130–2843) that is incapable of forming complexes with β-catenin, Axin, and GSK3β[22] into SW480 cells had no effect on both β-catenin phosphorylation and Flag-Hath1 protein stability (Figure 4*A*). This reciprocal regulation of Hath1 and β-catenin protein stability by Wnt signaling was also observed in 293T cells, in which Wnt signaling is usually inactivated. Activation of Wnt signaling in 293T cells by overexpression of the *Wnt1* gene resulted in a significant increase of the endogenous dephosphorylated, stabilized form of β-catenin protein and also a significant decrease in Flag-Hath1 protein expression. Treatment with MG132 or BIO completely restored the reduction of Flag-Hath1 protein expression induced by activation of Wnt signaling in 293T cells, suggesting that proteasome-mediated Hath1 proteolysis is regulated by the kinase activity of GSK-3β downstream of the canonical Wnt pathway (Figure 4*B*).

We further examined whether Wnt-GSK3β–mediated reciprocal regulation of Hath1 and β-catenin protein stability may also change the transcriptional activity of the corresponding downstream target genes of each protein. Consistent with previous reports,[22] expression of APC2 in SW480 cells decreased the ratio of TOPflash and FOPflash reporter activity by 0.14-fold, regardless of Flag-Hath1 cotransfection (Figure 4*C*). In sharp contrast, E-box–dependent reporter activity was increased by 2.3-fold by cotransfection of APC2 with Flag-Hath1 compared with single transfection of Flag-Hath1 into SW480 cells (Figure 4*C*). Thus, expression of APC2 in SW480 cells significantly down-regulated β-catenin/TCF–dependent transcription but conversely up-regulated Hath1-mediated, E-box–dependent transcription. In contrast, forced expression of *Wnt1* gene in 293T cells up-regulated the ratio of TOPflash and FOPflash reporter activity by 6-fold and, conversely, when Wnt1 was coexpressed with Flag-Hath1 in 293T cells, E-box–dependent reporter activity was down-regulated by 0.6-fold (Figure 4*D*). Thus, expression of Wnt1 in 293T cells significantly up-regulated β-catenin/TCF–dependent transcription but conversely down-regulated Hath1-mediated, E-box–dependent transcription. Single transfection of APC2 or Wnt1 does not change E-box–dependent transcription activity in both SW480 and 293T cells, suggesting that the observed E-box–dependent transcriptional activity represents Hath1-mediated transcription.

These data collectively indicated that GSK3β-mediated proteolysis of Hath1 protein observed in colon cancer cells is dependent on the aberrant activation of the canonical Wnt pathway and that GSK3β reciprocally regulates Hath1 and β-catenin protein stability in a Wnt-dependent manner, directly leading to significant changes in transcriptional activity of the downstream target genes.

Inactivation of Canonical Wnt Signaling Is Required for Hath1-Mediated Colonocyte Differentiation

It is well known that β-catenin/TCF–dependent transcription often promotes cell proliferation, whereas Hath1-dependent transcription promotes cell differentiation. Therefore, we next examined whether the Wnt-GSK3-mediated, reciprocal regulation of β-catenin and Hath1 protein stability and function may regulate the differentiation of colonocytes. For this purpose, we examined whether stabilization of Hath1 protein induced by inactivation of Wnt signaling may lead to spontaneous differentiation of poorly differentiated colon cancer cells. Consistent with former results, single transfection of APC2 into SW480 cells down-regulated mRNA expression of c-Myc but had no effect on colonocyte differentiation (Figure 5*A*). However, when Flag-Hath1 was cotransfected with APC2 in SW480 cells, Hath1 protein was stably expressed and subsequently induced expression of MUC2 mRNA, a specific marker for goblet cell differentiation.[35,36] Immunocytochemical analysis of Hath1 and MUC2 protein expression in SW480 cells showed that both stabilization of Flag-Hath1 protein and up-regulation of MUC2 protein expression were induced under the same condition (Figure 5*B*). Moreover, MUC2 protein was detected exclusively in green fluorescent protein–positive cells that were the bicistronic expression of *Flag-Hath1* gene, indicating that Hath1 protein caused the increase of MUC2 protein (Figure 5*B*).

Collectively, these results suggested that both inactivation of Wnt signaling and stable expression of Hath1

protein are required for colonocyte differentiation toward goblet cells.

A previous report showed that merely inactivating the aberrant Wnt signaling in HT-29 cells induced significant up-regulation of the *MUC2* gene.[19] In our experience, HT-29 cells are different from SW480 cells, because they readily express a small amount of Hath1 and MUC2 mRNA (data not shown). Thus, we speculate that inactivation of aberrant Wnt signaling in HT-29 cells may have up-regulated both mRNA expression and protein stability of the endogenous *Hath1* gene, leading to the significant up-regulation of MUC2 expression.

Hath1 Protein Expression Is Decreased in Human Colon Cancer Tissues Expressing Hath1 mRNA and Nuclear-Located β-catenin Protein

To reveal the role of Wnt-GSK3–mediated reciprocal proteolytic regulation of β-catenin and Hath1 in vivo, we analyzed the correlation between Hath1 mRNA, Hath1 protein, and nuclear localized β-catenin protein expression in human colon cancer tissues. In 3 of 4 cases, we found that tumor tissues expressed Hath1 mRNA at an amount comparable to the adjacent normal mucosa, as judged by RT-PCR (Figure 6*A*). Constitutive activation of Wnt signaling in cancer tissue of these cases was confirmed by the significant expression of *c-MYC*, one of the well-known target genes by β-catenin/TCF. Strikingly, in these cases, immunohistochemical analysis revealed that Hath1 protein is expressed in the normal mucosa but not in the tumor lesion (Figure 6*B*). In contrast, nuclear localized β-catenin protein was easily observed in the tumor lesion but was hardly found in the normal mucosa (Figure 6*B*). These data indicated that at least in some populations of colon cancers, Hath1 expression might be strictly suppressed by Wnt-mediated protein degradation, rather than the suppression of mRNA expression, thereby contributing to maintenance of the undifferentiated state of the tumor tissue.

Discussion

The present study describes a novel function of the canonical Wnt signaling, reciprocally regulating Hath1 and β-catenin protein stability via GSK3β (Figure 7). The "on" and "off" status of the Wnt signal directly converted the target of GSK3β between Hath1 and β-catenin protein, leading to subsequent protein degradation. Our results suggest that this mechanism not only regulates the amount of Hath1 and β-catenin protein expression but also contributes to the significant change in the expression of the downstream target genes and to the cell fate decision between cell differentiation and proliferation. Furthermore, our observations that the dysregulation of the Wnt pathway by components upstream of GSK3β, such as APC, not only contribute to the activation of β-catenin/TCF transcription but also induce concomitant destruction of the gut-specific transcription factor Hath1, provides new insights into the tissue-specific processes of colon cancer development.

It is known that the ubiquitin-proteasome pathway plays crucial roles in the carcinogenesis of some tissues by regulating the protein expression of transcriptional factors such as nuclear factor κB[37] and hypoxia-inducible factor 1.[38] However, our findings suggest that proteolytic regulation of Hath1 protein expression by the ubiquitin-proteasome pathway is a tissue-specific event observed exclusively in colon cancer cells. Moreover, the present system has an outstanding advantage for colon cancer carcinogenesis, in that a single mutation of an upstream gene in Wnt signaling could accelerate cell proliferation by β-catenin/TCF–dependent transcription and immediately shut down cell differentiation at the same time by rapid degradation of Hath1 protein, regardless of Hath1 mRNA expression. Therefore, the present function of the Wnt-GSK pathway further emphasizes the importance of aberrant Wnt signaling in colonocyte transformation.

This study also provides a new insight into the canonical Wnt pathway, because it indicates that GSK3β functions continuously, even when the upstream signal is inactivated, by changing its substrate specificity according to the upstream signal status. It is known that GSK3β changes target amino acid residue within a single substrate protein such as Map1b[39] and Snail,[40] depending on its upstream signals. Our study suggests for the first time that GSK3β could even change the substrate protein itself due to upstream Wnt signaling, leading to immediate degradation of the substrate protein by the ubiquitin-proteasome system. However, the present study could not provide precise evidence to understand whether Hath1 is directly phosphorylated by GSK3β or how changes of GSK3β target are sequentially regulated between Hath1 and β-catenin. In our recent study, in vitro kinase assay using recombinant Hath1 protein and activated GSK3β did not show any phosphorylation of Hath1 protein (data not shown). This result indicated that the phosphorylation of Hath1 might require specific adapter proteins such as Axin and APC to form a complex with GSK3β, as is the case with phosphorylation of β-catenin. However, so far we cannot completely exclude that the effect of GSK3β activity on Hath1 protein stability is possibly indirect. Overexpression of GSK3β had no effect on Hath1 and β-catenin protein stability, suggesting that the total amount of GSK3β protein is abundant enough and does not contribute to limit the substrate protein (data not shown). Thus, it is more likely that Wnt signal controls target specificity of the GSK3β by regulating the complex formation of the substrate with GSK3β and a yet-unknown adapter protein.

In summary, we showed for the first time a novel function of the Wnt-GSK3 signaling pathway, working as a molecular switch changing the cell fate between differentiation and proliferation by proteolytic, reciprocal reg-

ulation of Hath1 and β-catenin in colonocytes. Moreover, the aberrant Wnt signaling contributes to the carcinogenesis of colon cancers not only by the stabilization of β-catenin protein but also by the degradation of Hath1 protein in an intestine-specific manner. These findings provide better understanding of the molecular mechanism regulating Wnt-mediated carcinogenesis in colorectal cancers and further emphasize the importance of aberrant Wnt signaling in colonocyte transformation.

References

1. Booth C, Brady G, Potten CS. Crowd control in the crypt. Nat Med 2002;8:1360–1361.
2. El-Assal ON, Besner GE. HB-EGF enhances restitution after intestinal ischemia/reperfusion via PI3K/Akt and MEK/ERK1/2 activation. Gastroenterology 2005;129:609–625.
3. Haramis AP, Begthel H, van den Born M, van Es J, Jonkheer S, Offerhaus GJ, Clevers H. De novo crypt formation and juvenile polyposis on BMP inhibition in mouse intestine. Science 2004; 303:1684–1686.
4. Cheng H, Leblond CP. Origin, differentiation and renewal of the four main epithelial cell types in the mouse small intestine. V. Unitarian theory of the origin of the four epithelial cell types. Am J Anat 1974;141:537–561.
5. Gowan K, Helms AW, Hunsaker TL, Collisson T, Ebert PJ, Odom R, Johnson JE. Crossinhibitory activities of Ngn1 and Math1 allow specification of distinct dorsal interneurons. Neuron 2001;31: 219–232.
6. Ben-Arie N, Bellen HJ, Armstrong DL, McCall AE, Gordadze PR, Guo Q, Matzuk MM, Zoghbi HY. Math1 is essential for genesis of cerebellar granule neurons. Nature 1997;390:169–172.
7. Leonard JH, Cook AL, Van Gele M, Boyle GM, Inglis KJ, Speleman F, Sturm RA. Proneural and proneuroendocrine transcription factor expression in cutaneous mechanoreceptor (Merkel) cells and Merkel cell carcinoma. Int J Cancer 2002;101:103–110.
8. Bermingham NA, Hassan BA, Price SD, Vollrath MA, Ben-Arie N, Eatock RA, Bellen HJ, Lysakowski A, Zoghbi HY. Math1: an essential gene for the generation of inner ear hair cells. Science 1999;284:1837–1841.
9. Yang Q, Bermingham NA, Finegold MJ, Zoghbi HY. Requirement of Math1 for secretory cell lineage commitment in the mouse intestine. Science 2001;294:2155–2158.
10. Fre S, Huyghe M, Mourikis P, Robine S, Louvard D, Artavanis-Tsakonas S. Notch signals control the fate of immature progenitor cells in the intestine. Nature 2005;435:964–968.
11. Jensen J, Pedersen EE, Galante P, Hald J, Heller RS, Ishibashi M, Kageyama R, Guillemot F, Serup P, Madsen OD. Control of endodermal endocrine development by Hes-1. Nat Genet 2000; 24:36–44.
12. Sekine A, Akiyama Y, Yanagihara K, Yuasa Y. Hath1 up-regulates gastric mucin gene expression in gastric cells. Biochem Biophys Res Commun 2006;344:1166–1171.
13. Batlle E, Henderson JT, Beghtel H, van den Born MM, Sancho E, Huls G, Meeldijk J, Robertson J, van de Wetering M, Pawson T, Clevers H. Beta-catenin and TCF mediate cell positioning in the intestinal epithelium by controlling the expression of EphB/ephrinB. Cell 2002;111:251–263.
14. Huelsken J, Behrens J. The Wnt signalling pathway. J Cell Sci 2002;115:3977–3978.
15. Polakis P. Wnt signaling and cancer. Genes Dev 2000;14:1837–1851.
16. Marshman E, Booth C, Potten CS. The intestinal epithelial stem cell. Bioessays 2002;24:91–98.
17. Pinto D, Gregorieff A, Begthel H, Clevers H. Canonical Wnt signals are essential for homeostasis of the intestinal epithelium. Genes Dev 2003;17:1709–1713.
18. Polakis P. The oncogenic activation of beta-catenin. Curr Opin Genet Dev 1999;9:15–21.
19. Leow CC, Romero MS, Ross S, Polakis P, Gao WQ. Hath1, down-regulated in colon adenocarcinomas, inhibits proliferation and tumorigenesis of colon cancer cells. Cancer Res 2004;64: 6050–6057.
20. Shimura H, Hattori N, Kubo S, Mizuno Y, Asakawa S, Minoshima S, Shimizu N, Iwai K, Chiba T, Tanaka K, Suzuki T. Familial Parkinson disease gene product, parkin, is a ubiquitin-protein ligase. Nat Genet 2000;25:302–305.
21. Onishi M, Kinoshita S, Morikawa Y, Shibuya A, Phillips J, Lanier LL, Gorman DM, Nolan GP, Miyajima A, Kitamura T. Applications of retrovirus-mediated expression cloning. Exp Hematol 1996; 24:324–329.
22. Munemitsu S, Albert I, Souza B, Rubinfeld B, Polakis P. Regulation of intracellular beta-catenin levels by the adenomatous polyposis coli (APC) tumor-suppressor protein. Proc Natl Acad Sci U S A 1995;92:3046–3050.
23. Nishita M, Hashimoto MK, Ogata S, Laurent MN, Ueno N, Shibuya H, Cho KW. Interaction between Wnt and TGF-beta signalling pathways during formation of Spemann's organizer. Nature 2000;403:781–785.
24. Oshima S, Nakamura T, Namiki S, Okada E, Tsuchiya K, Okamoto R, Yamazaki M, Yokota T, Aida M, Yamaguchi Y, Kanai T, Handa H, Watanabe M. Interferon regulatory factor 1 (IRF-1) and IRF-2 distinctively up-regulate gene expression and production of interleukin-7 in human intestinal epithelial cells. Mol Cell Biol 2004; 24:6298–6310.
25. Matsumoto T, Okamoto R, Yajima T, Mori T, Okamoto S, Ikeda Y, Mukai M, Yamazaki M, Oshima S, Tsuchiya K, Nakamura T, Kanai T, Okano H, Inazawa J, Hibi T, Watanabe M. Increase of bone marrow-derived secretory lineage epithelial cells during regeneration in the human intestine. Gastroenterology 2005;128:1851–1867.
26. Akazawa C, Ishibashi M, Shimizu C, Nakanishi S, Kageyama R. A mammalian helix-loop-helix factor structurally related to the product of Drosophila proneural gene atonal is a positive transcriptional regulator expressed in the developing nervous system. J Biol Chem 1995;270:8730–8738.
27. Ciechanover A. The ubiquitin-proteasome proteolytic pathway. Cell 1994;79:13–21.
28. Hochstrasser M. Ubiquitin-dependent protein degradation. Annu Rev Genet 1996;30:405–439.
29. Massari ME, Murre C. Helix-loop-helix proteins: regulators of transcription in eucaryotic organisms. Mol Cell Biol 2000;20: 429–440.
30. Roos-Mattjus P, Sistonen L. The ubiquitin-proteasome pathway. Ann Med 2004;36:285–295.
31. Weissman AM. Themes and variations on ubiquitylation. Nat Rev Mol Cell Biol 2001;2:169–178.
32. Cross DA, Alessi DR, Cohen P, Andjelkovich M, Hemmings BA. Inhibition of glycogen synthase kinase-3 by insulin mediated by protein kinase B. Nature 1995;378:785–789.
33. Doble BW, Woodgett JR. GSK-3: tricks of the trade for a multitasking kinase. J Cell Sci 2003;116:1175–1186.
34. Zeng X, Tamai K, Doble B, Li S, Huang H, Habas R, Okamura H, Woodgett J, He X. A dual-kinase mechanism for Wnt co-receptor phosphorylation and activation. Nature 2005;438:873–877.
35. Chang SK, Dohrman AF, Basbaum CB, Ho SB, Tsuda T, Toribara NW, Gum JR, Kim YS. Localization of mucin (MUC2 and MUC3) messenger RNA and peptide expression in human normal intestine and colon cancer. Gastroenterology 1994;107:28–36.
36. Katz JP, Perreault N, Goldstein BG, Lee CS, Labosky PA, Yang VW, Kaestner KH. The zinc-finger transcription factor Klf4 is

required for terminal differentiation of goblet cells in the colon. Development 2002;129:2619–2628.
37. Greten FR, Eckmann L, Greten TF, Park JM, Li ZW, Egan LJ, Kagnoff MF, Karin M. IKK beta links inflammation and tumorigenesis in a mouse model of colitis-associated cancer. Cell 2004; 118:285–296.
38. Koshiji M, Kageyama Y, Pete EA, Horikawa I, Barrett JC, Huang LE. HIF-1 alpha induces cell cycle arrest by functionally counteracting Myc. EMBO J 2004;23:1949–1956.
39. Trivedi N, Marsh P, Goold RG, Wood-Kaczmar A, Gordon-Weeks PR. Glycogen synthase kinase-3 beta phosphorylation of MAP1B at Ser1260 and Thr1265 is spatially restricted to growing axons. J Cell Sci 2005;118:993–1005.
40. Zhou BP, Deng J, Xia W, Xu J, Li YM, Gunduz M, Hung MC. Dual regulation of Snail by GSK-3beta-mediated phosphorylation in control of epithelial-mesenchymal transition. Nat Cell Biol 2004; 6:931–940.

Received May 17, 2006. Accepted October 5, 2006.

Address requests for reprints to: Mamoru Watanabe, MD, PhD, Department of Gastroenterology and Hepatology, Graduate School, Tokyo Medical and Dental University, 1-5-45, Yushima, Bunkyo-ku, Tokyo 113-8519, Japan. e-mail: mamoru.gast@tmd.ac.jp.

Supported in part by grants-in-aid for Scientific Research, Scientific Research on Priority Areas, Exploratory Research, and Creative Scientific Research from the Japanese Ministry of Education, Culture, Sports, Science and Technology; the Japanese Ministry of Health, Labor and Welfare; the Japan Medical Association; the Foundation for Advancement of International Science; Terumo Life Science Foundation; Ohyama Health Foundation; Yakult Bio-Science Foundation; and the Research Fund of Mitsukoshi Health and Welfare Foundation.

The authors thank Dr Akira Kikuchi (Hiroshima University), Dr Hiroshi Shibuya (Tokyo Medical and Dental University), and Dr Keiji Tanaka (Tokyo Metropolitan Institute) for technical advice.

Systemic, but Not Intestinal, IL-7 Is Essential for the Persistence of Chronic Colitis[1]

Takayuki Tomita, Takanori Kanai,[2] Yasuhiro Nemoto, Teruji Totsuka, Ryuichi Okamoto, Kiichiro Tsuchiya, Naoya Sakamoto, and Mamoru Watanabe

We previously demonstrated that IL-7 is produced by intestinal goblet cells and is essential for the persistence of colitis. It is well known, however, that goblet cells are decreased or depleted in the chronically inflamed mucosa of animal colitis models or human inflammatory bowel diseases. Thus, in this study, we assess whether intestinal IL-7 is surely required for the persistence of colitis using a RAG-1/2$^{-/-}$ colitis model induced by the adoptive transfer of CD4$^+$CD45RB^{high} T cells in combination with parabiosis system. Surprisingly, both IL-7$^{-/-}$ × RAG-1$^{-/-}$ and IL-7$^{+/+}$ × RAG-1$^{-/-}$ host mice developed colitis 4 wk after parabiosis to a similar extent of colitic IL-7$^{+/+}$ × RAG-1$^{-/-}$ donor mice that were previously transferred with CD4$^+$CD45RB^{high} T cells. Of note, although the number of CD4$^+$ T cells recovered from the spleen or the bone marrow of IL-7$^{-/-}$ × RAG-1$^{-/-}$ host mice was significantly decreased compared with that of IL-7$^{+/+}$ × RAG-1$^{-/-}$ host mice, an equivalent number of CD4$^+$ T cells was recovered from the lamina propria of both mice, indicating that the expansion of CD4$^+$ T cells in the spleen or in the bone marrow is dependent on IL-7, but not in the lamina propria. Development of colitis was never observed in parabionts between IL-7$^{+/+}$ × RAG-1$^{-/-}$ host and noncolitic IL-7$^{-/-}$ × RAG-1$^{-/-}$ donor mice that were transferred with CD4$^+$CD45RB^{high} T cells. Collectively, systemic, but not intestinal, IL-7 is essential for the persistence of colitis, suggesting that therapeutic approaches targeting the systemic IL-7/IL-7R signaling pathway may be feasible in the treatment of inflammatory bowel diseases. *The Journal of Immunology*, 2008, 180: 383–390.

Inflammatory bowel disease (IBD)[3] are caused by chronic inflammatory responses in the gut wall, commonly take persistent courses, but in some patients relapse after remissions (1–6). Because the recurrent disease usually mimics the primary disease episode, it is possible that the disease is caused by the repeated activation and expansion of colitogenic effector CD4$^+$ T cells arising from common long-lived colitogenic memory CD4$^+$ T cells, which latently reside in their target tissues or in some reservoirs. Nevertheless, the nature of the colitogenic memory CD4$^+$ T cells over time is not fully understood.

IL-7 is secreted by stromal cells in the bone marrow (BM) and thymus, and epithelial cells including the intestine (7–10). Recent findings revealed that IL-7 is an important cytokine supporting the survival of resting naive and memory CD4$^+$ T cells, but not effector CD4$^+$ T cells (9–16). We have previously demonstrated that, 1) IL-7 is constitutively produced by intestinal goblet epithelial cells (8), 2) IL-7 transgenic (Tg) mice, in which IL-7 overexpression was driven by SRα promotor, developed chronic colitis that mimicked histopathological characteristics of human IBD (17), 3) mucosal CD4$^+$IL-7Rα^{high} T cells in CD4$^+$CD45RB^{high} T cell-transferred colitic mice are colitogenic (18), and 4) IL-7$^{-/-}$ × RAG-1$^{-/-}$ mice transferred with colitogenic lamina propria (LP) CD4$^+$ T cells isolated from colitic CD4$^+$CD45RB^{high} T cell-transferred mice did not develop colitis (19).

Somewhat at odds, however, we also found that production of intestinal IL-7 was dramatically decreased in the inflamed mucosa of colitic IL-7 Tg mice in accordance with depletion of goblet cells (17). Because our IL-7 Tg mice were established by expressing IL-7 under regulation of the ubiquitous SRα promoter, it was possible that intestinal IL-7 is indeed decreased at the site of mucosal inflammation due to depletion of goblet cells, which is a feature often seen in the inflamed mucosa of human IBD, but systemic IL-7 of other tissue origin, such as BM (20) and thymus (21), is rather critical for the maintenance of colitogenic memory CD4$^+$ T cells. Based on these complex backgrounds, in this study, we assess the distinct requirement of intestinal or systemic IL-7 in the development and persistence of colitis using a RAG-1/2$^{-/-}$ colitis model (22, 23) induced by adoptive transfer of CD4$^+$CD45RB^{high} T cells in combination with parabiosis system.

Materials and Methods

Animals

C57BL/6-Ly5.2 mice were purchased from Japan CLEA. C57BL/6-Ly5.1 mice and C57BL/6-Ly5.2-RAG-2-deficient (RAG-2$^{-/-}$) mice were obtained from Taconic Farms and Central Laboratories for Experimental Animals. C57BL/6-Ly5.2-background RAG-1$^{+/-}$ and IL-7$^{+/-}$ mice were provided from Dr. Rosa Zamoyska (National Institute for Medical Research, London, U.K.) (24). These mice were intercrossed to generate IL-7$^{-/-}$ × RAG-1$^{-/-}$ and IL-7$^{+/+}$ × RAG-1$^{-/-}$ littermate mice in the Animal Care Facility of Tokyo Medical and Dental University (TMDU). Mice were maintained under specific pathogen-free conditions in the Animal Care Facility of TMDU. Donors and recipients were used at 6–12 wk of

Department of Gastroenterology and Hepatology, Graduate School, Tokyo Medical and Dental University, Tokyo, Japan

Received for publication June 14, 2007. Accepted for publication October 29, 2007.

The costs of publication of this article were defrayed in part by the payment of page charges. This article must therefore be hereby marked *advertisement* in accordance with 18 U.S.C. Section 1734 solely to indicate this fact.

[1] This study was supported in part by grants-in-aid for Scientific Research, Scientific Research on Priority Areas, Exploratory Research and Creative Scientific Research from the Japanese Ministry of Education, Culture, Sports, Science and Technology; the Japanese Ministry of Health, Labor and Welfare; the Japan Medical Association; Foundation for Advancement of International Science; Terumo Life science Foundation; Ohyama Health Foundation; Yakult Bio-Science Foundation; and Research Fund of Mitsukoshi Health and Welfare Foundation.

[2] Address correspondence and reprint requests to Dr. Takanori Kanai, Department of Gastroenterology and Hepatology, Tokyo Medical and Dental University, 1-5-45 Yushima, Bunkyo-ku, Tokyo 113-8519, Japan. E-mail address: taka.gast@tmd.ac.jp

[3] Abbreviations used in this paper: IBD, inflammatory bowel disease; BM, bone marrow; LP, lamina propria; SP, spleen; Tg, transgenic; IEL, intraepithelial cell; HPF, high power field; DAPI, 4′, 6′-diamidino-2-phenylindole; LN, lymph node.

 0022-1767/07/$2.00

age. All experiments were approved by the regional animal study committees and were done according to institutional guidelines and Home Office regulations.

Parabiosis experimental design

To assess the specific requirement of mucosal or systemic IL-7 in the development of colitis, we performed adoptive transfer experiment in combination with a parabiosis system using IL-$7^{+/+}$ × RAG-$1^{-/-}$ and IL-$7^{-/-}$ × RAG-$1^{-/-}$ littermate recipients (Fig. 1*A*). For adoptive transfer, $CD4^+$ T cells were first isolated from SP cells of C57BL/6-Ly5.2 mice using the anti-CD4 (L3T4)-MACS system (Miltenyi Biotec) according to the manufacturer's instruction. Enriched $CD4^+$ T cells (96–97% pure, as estimated by FACSCalibur (BD Biosciences)) were then labeled with PE-conjugated anti-mouse CD4 (RM4–5; BD Pharmingen) and FITC-conjugated anti-mouse (16A; BD Pharmingen). $CD4^+CD45RB^{high}$ cells were purified using a FACSAria (BD Biosciences). This population was >98.0% pure on reanalysis. IL-$7^{+/+}$ × RAG-$1^{-/-}$ mice (n = 18) and IL-$7^{-/-}$ × RAG-$1^{-/-}$ mice (n = 6) were then injected i.p. with 3×10^5 splenic $CD4^+CD45RB^{high}$ T cells from normal C57BL/6-Ly5.2 mice. After 6 wk post transfer, IL-$7^{+/+}$ × RAG-$1^{-/-}$ mice, but not IL-$7^{-/-}$ × RAG-$1^{-/-}$ mice, transferred with $CD4^+CD45RB^{high}$ T cells developed a wasting disease and colitis as previously reported (19).

We then conducted parabiosis surgery according to institutional guidelines and Home Office regulations. In brief, sex-matched mice were anesthetized before surgery, and incisions were made in the skin on the opposing flanks of the donor and recipient animals. Surgical sutures were used to bring the body walls of the two mice into direct physical contact. The outer skin was then attached with surgical staples. For this parabiosis experiment, we divided colitic IL-$7^{+/+}$ × RAG-$1^{-/-}$ (n = 18) mice that were previously transferred with $CD4^+CD45RB^{high}$ T cells into three groups: Group 1, colitic IL-$7^{+/+}$ × RAG-$1^{-/-}$ mice joined with normal C57BL/6-Ly5.1 mice (n = 6); Group 2, colitic IL-$7^{+/+}$ × RAG-$1^{-/-}$ mice joined with new IL-$7^{+/+}$ × RAG-$1^{-/-}$ mice (n = 6); Group 3, colitic IL-$7^{+/+}$ × RAG-$1^{-/-}$ mice joined with new IL-$7^{-/-}$ × RAG-$1^{-/-}$ mice (n = 6). As Group 4, noncolitic IL-$7^{-/-}$ × RAG-$1^{-/-}$ mice previously transferred with $CD4^+CD45RB^{high}$ T cells were joined with new IL-$7^{+/+}$ × RAG-$1^{-/-}$ mice (n = 6). All mice were observed for clinical signs, such as hunched posture, piloerection, diarrhea, and blood in the stool. At autopsy, mice were assessed for a clinical score (25) that is the sum of three parameters as follows: hunching and wasting, 0 or 1; colon thickening, 0–3 (0, no colon thickening; 1, mild thickening; 2, moderate thickening; 3, extensive thickening); and stool consistency, 0–3 (0, normal beaded stool; 1, soft stool; 2, diarrhea; 3, bloody stool) (25).

Histological examination

Tissue samples were fixed in PBS containing 10% neutral-buffered formalin. Paraffin-embedded sections (5 μm) were stained with H&E. Three tissue samples from the proximal, middle, and distal parts of the colon were prepared. The sections were analyzed without prior knowledge of each mouse. The area most affected was graded by the number and severity of lesions. The mean degree of inflammation in the colon was calculated using a modification of a previously described scoring system (25) as follows: mucosa damage, 0; normal, 1; 3–10 intraepithelial cells (IEL)/high power field (HPF) and focal damage, 2; >10 IEL/HPF and rare crypt abscesses, 3; >10 IEL/HPF, multiple crypt abscesses and erosion/ulceration, submucosa damage, 0; normal or widely scattered leukocytes, 1; focal aggregates of leukocytes, 2; diffuse leukocyte infiltration with expansion of submucosa, 3; diffuse leukocyte infiltration, muscularis damage, 0; normal or widely scattered leukocytes, 1; widely scattered leukocyte aggregates between muscle layers, 2; leukocyte infiltration with focal effacement of the muscularis, 3; extensive leukocyte infiltration with transmural effacement of the muscularis.

Tissue preparations

Single cell suspensions were prepared from SP, LP, and BM as previously described (18). To isolate LP $CD4^+$ T cells, the entire length of the colon was opened longitudinally, washed with PBS, and cut into small pieces. The dissected mucosa was incubated with Ca^{2+}, Mg^{2+}-free HBSS containing 1 mM DTT (Sigma-Aldrich) for 45 min to remove mucus and then treated with 3.0 mg/ml collagenase (Roche) and 0.01% DNase (Worthington Biochemical) for 2 h. The cells were pelleted two times through a 40% isotonic Percoll solution, and then subjected to Ficoll-Hypaque density gradient centrifugation (40/75%). Enriched LP $CD4^+$ T cells were obtained by positive selection using anti-CD4 (L3T4) MACS magnetic beads. The resultant cells when analyzed by FACSCalibur contained >95% $CD4^+$ cells. BM cells were obtained by flushing two femurs with cold RPMI 1640. For in vitro assay, only live cells were counted by using trypan blue staining method, and confirmed that the viability of cells was almost the same (>96% live) among the sample groups.

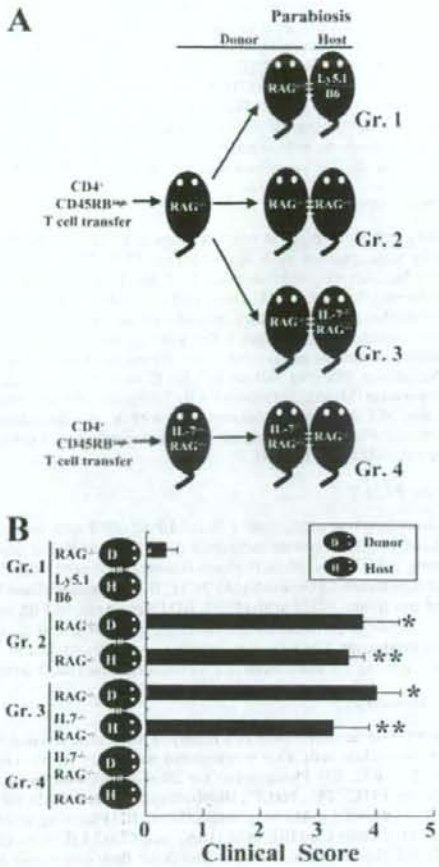

FIGURE 1. Host IL-$7^{-/-}$ × RAG-$1^{-/-}$ mice in parabionts with diseased IL-$7^{+/+}$ × RAG-$1^{-/-}$ donor mice show a wasting disease and clinical signs of colitis. *A*, Parabiosis experimental design. For an adoptive transfer, splenic $CD4^+CD45RB^{high}$ T cells were isolated from C57BL/6-Ly5.2 mice, and then transferred into female IL-$7^{+/+}$ × RAG-$1^{-/-}$ mice (n = 18) and IL-$7^{-/-}$ × RAG-$1^{-/-}$ mice (n = 6). Six wk after transfer, IL-$7^{+/+}$ × RAG-$1^{-/-}$, but not IL-$7^{-/-}$ × RAG-$1^{-/-}$, mice transferred with $CD4^+CD45RB^{high}$ T cells developed a wasting disease and colitis. As parabiosis pairs, Group 1 parabionts were joined between colitic donor IL-$7^{+/+}$ × RAG-$1^{-/-}$ mice and normal host C57BL/6-Ly5.1 mice (n = 6 pairs). Group 2 parabionts were joined between colitic donor IL-$7^{+/+}$ × RAG-$1^{-/-}$ mice and new host IL-$7^{+/+}$ × RAG-$1^{-/-}$ mice (n = 6 pairs). Group 3 parabionts were joined between colitic donor IL-$7^{+/+}$ × RAG-$1^{-/-}$ mice and new host IL-$7^{-/-}$ × RAG-$1^{-/-}$ mice (n = 6 pairs). Group 4 parabionts were joined between noncolitic donor IL-$7^{-/-}$ × RAG-$1^{-/-}$ mice and new host IL-$7^{+/+}$ × RAG-$1^{-/-}$ mice (n = 6 pairs). Jointed animals were maintained for 4 wk after surgery. Gr. 1, Group 1; Gr. 2, Group 2; Gr. 3, Group 3; and Gr. 4, Group 4. *B*, Clinical scores were determined at 4 wk after surgery as described in *Materials and Methods*. Data are indicated as mean ± SEM of six mice in each group. *, $p < 0.01$, vs Group 1 donor mice. **, $p < 0.01$, vs Group 1 host mice.

Reverse transcription polymerase chain reaction

Total RNA was isolated by using Isogen reagent (Nippon Gene). Aliquots of 5 μg total RNA were used for complementary DNA synthesis in a reaction volume of 20 μl using random primers. One microliter of reverse transcription product was amplified with 0.25 U of rTaq DNA polymerase

(Toyoba) in a 50 μl reaction. Sense and antisense primers and the cycle numbers for the amplification of each gene were as follows: sense IL-7, 5′-GCCTGTCACATCATCTGAGTGCC-3′ and antisense IL-7, 5′-CAG GAGGCATCCAGGAACTTCTG-3′ for IL-7 (35 cycles); and sense G3PDH, 5′-TGAAGGTCGGTGTGAACGGATTTGGC-3′ and antisense G3PDH, 5′-CATGTAGGCCATGAGGTCCACCAC-3′ for G3PDH (30 cycles). The amplification for each gene was logarithmic under these conditions. PCR products were separated on 1.8% agarose gels, stained with ethidium bromide, and visualized with a Lumi-Imager F1 (Roche).

Immunohistochemistry

We used consecutive cryostat colon sections in all studies. Immunohistochemistry using purified mAb against mouse CD4 (RM4–5; BD Pharmingen) or biotin-conjugated polyclonal IL-7 Ab (BAF407; R&D Systems) was performed. In brief, O.C.T. compound-embedded tissue samples were cut into serial sections 6-μm thick, placed on coated slides, and fixed with 4% paraformaldehyde phosphate buffer solution for 10 min. Slides were then incubated with the primary Ab at 4°C overnight, followed by staining with AlexaFluor 488 goat anti-rat IgG for CD4 detection or AlexaFluor 488 streptavidin (Molecular Probes) for IL-7 detection at room temperature for 60 min. All slides were counterstained with 4′, 6′ -diamidino-2-phenylindole (DAPI; Vector Laboratories) and observed under a confocal microscopy (LSM510 Carl Zeiss).

Cytokine ELISA

To measure cytokine production, 1×10^5 LP $CD4^+$ T cells were cultured in triplicate of 200 μl culture medium at 37°C in a humidified atmosphere containing 5% CO_2 in 96-well plates (Costar) precoated with 5 μg/ml hamster anti-mouse CD3ε mAb (145-2C11, BD Pharmingen) and hamster 2 μg/ml anti-mouse CD28 mAb (37.51, BD Pharmingen) in PBS overnight at 4°C. Culture supernatants were collected after 48 h and assayed for cytokine production. Cytokine concentrations were determined by specific ELISA following the manufacturer's recommendation (R&D Systems).

Flow cytometry

To detect the surface expression of a variety of molecules, isolated SP, BM, or LP mononuclear cells were preincubated with an FcγR-blocking mAb (CD16/32; 2.4G2, BD Pharmingen) for 20 min followed by incubation with specific FITC-, PE-, PerCP-, allophycocyanin-labeled Abs for 30 min on ice. The following mAbs were obtained from BD Pharmingen: anti-CD4 mAb (RM4–5), anti-CD45RB mAb (16A), anti-CD45.1 (Ly5.1; A20), and anti-CD45.2 (Ly5.2; 104). Standard four-color flow cytometric analyses were obtained using the FACSCalibur and analyzed by CellQuest software. Background fluorescence was assessed by staining with control irrelevant isotype-matched mAbs.

Statistical analysis

The results are expressed as mean ± SEM. Groups of data were compared by the Mann-Whitney U test. Differences were considered to be statistically significant when $p < 0.05$.

Results

IL-7$^{-/-}$ × RAG-1$^{-/-}$ host mice joined with colitic IL-7$^{+/+}$ × RAG-1$^{-/-}$ donor mice develop a wasting disease

We have previously demonstrated that IL-7 is essential for the development and the persistence of colitis as a survival factor for colitogenic $CD4^+$ memory T cells (19). Furthermore, we have found that IL-7 Tg mice, in which IL-7 was systemically overproduced, develop colitis spontaneously, but production of intestinal IL-7 was conversely decreased in the inflamed mucosa because of depletion of the goblet cells. Based on such paradoxical findings, in this study, we assess whether intestinal or systemic IL-7 is essential for the perpetuation of colitis, by adoptive transfer experiment in combination with parabiosis system using IL-7$^{+/+}$ × RAG-1$^{-/-}$ and IL-7$^{-/-}$ × RAG-1$^{-/-}$ littermate recipients (Fig. 1*A*). To this end, we first induced chronic colitis by adoptive transfer of splenic $CD4^+CD45RB^{high}$ T cells from normal C57BL/6-Ly5.2 mice into IL-7$^{+/+}$ × RAG-1$^{-/-}$ mice (Fig. 1*A*). Consistent with our previous report (19), the transferred IL-7$^{+/+}$ × RAG-1$^{-/-}$ mice manifested progressive weight loss from 3 wk after transfer and clinical symptoms of colitis 6 wk after transfer (data not shown). In contrast, the $CD4^+CD45RB^{high}$ T cell-transferred IL-7$^{-/-}$ × RAG-1$^{-/-}$ mice showed no clinical signs of colitis and weight loss (data not shown) (19), indicating that IL-7 is essential for the development of colitis.

At 6 wk after transfer, we next generated four groups of parabionts (Fig. 1*A*). In parabionts between colitic IL-7$^{+/+}$ × RAG-1$^{-/-}$ donor mice that has been previously transferred with $Ly5.2^+CD4^+CD45RB^{high}$ T cells and normal C57BL/6-Ly5.1 host mice (Group 1) (Fig. 1*A*), clinical symptoms, such as diarrhea, anorectal prolapse, and hunched posture, gradually decreased over time in IL-7$^{+/+}$ × RAG-1$^{-/-}$ donor mice as compared with the mice at the time of surgery, and completely disappeared at 4 wk after surgery by assessing the clinical score (Fig. 1*B*). C57BL/6-Ly5.1 host mice were consistently healthy during the observed period (Fig. 1*B*). In parabionts between colitic IL-7$^{+/+}$ × RAG-1$^{-/-}$ donor mice and new IL-7$^{+/+}$ × RAG-1$^{-/-}$ host mice (Group 2) (Fig. 1*A*), all the IL-7$^{+/+}$ × RAG-1$^{-/-}$ donor mice were consistently diseased (Fig. 1*B*), and clinical symptoms of colitis gradually increased in new IL-7$^{+/+}$ × RAG-1$^{-/-}$ host mice, which reached to the equal level of the paired IL-7$^{+/+}$ × RAG-1$^{-/-}$ donor mice at 4 wk after surgery (Fig. 1*B*). In parabionts between colitic IL-7$^{+/+}$ × RAG-1$^{-/-}$ donor mice and new IL-7$^{-/-}$ × RAG-1$^{-/-}$ host mice (Group 3) (Fig. 1*A*), IL-7$^{+/+}$ × RAG-1$^{-/-}$ donor mice remained diseased to a similar level of IL-7$^{+/+}$ × RAG-1$^{-/-}$ donor mice in Group 2 (Fig. 1*B*), and notably, IL-7$^{-/-}$ × RAG-1$^{-/-}$ host mice, albeit with the absence of intestinal IL-7, were gradually sick and clinical symptoms of colitis reached to the equal level of paired IL-7$^{+/+}$ × RAG-1$^{-/-}$ donor mice and the IL-7$^{+/+}$ × RAG-1$^{-/-}$ host mice in Group 2 at 4 wk after surgery (Fig. 1*B*). In sharp contrast, in parabionts between the nondiseased IL-7$^{-/-}$ × RAG-1$^{-/-}$ donor mice that were transferred with $CD4^+CD45RB^{high}$ T cells and new IL-7$^{+/+}$ × RAG-1$^{-/-}$ host mice (Group 4) (Fig. 1*A*), both IL-7$^{-/-}$ × RAG-1$^{-/-}$ donor and IL-7$^{+/+}$ × RAG-1$^{-/-}$ host mice were consistently healthy during the observed period (Fig. 1*B*), indicating that $CD4^+CD45RB^{high}$ T cell-transferred IL-7$^{-/-}$ × RAG-1$^{-/-}$ mice never retained colitogenic $CD4^+$ T cells.

IL-7$^{-/-}$ × RAG-1$^{-/-}$ host mice parabiosed with colitic IL-7$^{+/+}$ × RAG-1$^{-/-}$ donor mice develop Th1-mediated colitis

Four wk after surgery, the colons from parabionts between IL-7$^{+/+}$ × RAG-1$^{-/-}$ donor mice and C57BL/6-Ly5.1 host mice in Group 1 and parabionts between IL-7$^{-/-}$ × RAG-1$^{-/-}$ donor mice and IL-7$^{+/+}$ × RAG-1$^{-/-}$ host mice in Group 4 were macroscopically normal (data not shown). In contrast, the colon from all mice in Groups 2 and 3, regardless of IL-7$^{+/+}$ × RAG-1$^{-/-}$ or IL-7$^{+/+}$ × RAG-1$^{-/-}$ mice and as donors or hosts, were equally enlarged and had a greatly thickened wall (data not shown). In addition, the enlargement of spleen was also present in donors and hosts of Groups 2 and 3 mice (data not shown). Histological examination showed that in colons from Group 1, donor IL-7$^{+/+}$ × RAG-1$^{-/-}$ mice, which initially had clinical symptoms of colitis, exhibited no pathological change 4 wk after surgery, and were indistinguishable from the colons of C57BL/6-Ly5.1 host mice (Fig. 2*A*, *left*). In turn, we could not detect any pathological finding in Group 4 parabionts between IL-7$^{-/-}$ × RAG-1$^{-/-}$ donor mice and IL-7$^{+/+}$ × RAG-1$^{-/-}$ host mice. In contrast, all the donor and host mice in Groups 2 and 3 parabionts showed prominent epithelial hyperplasia with glandular elongation and a massive infiltration of mononuclear cells (Fig. 2*A*, *left*). This difference was also confirmed by histological scoring of colon sections (Fig. 2*B*), showing that the host mice in parabionts in Groups 2 and 3 developed colitis comparable to the paired diseased donor mice that had sustained colitis, while all the donor and host mice in Groups

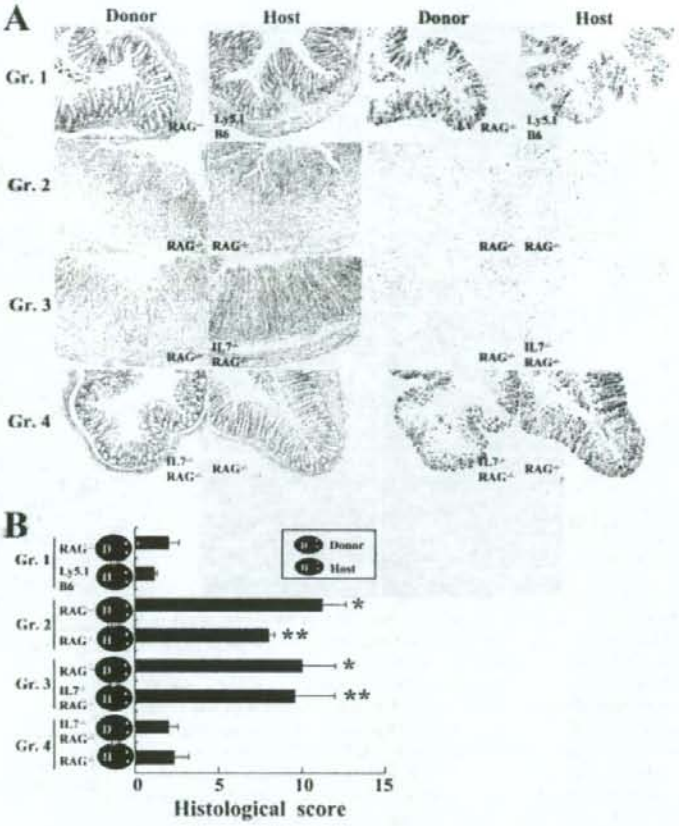

FIGURE 2. IL-$7^{-/-}$ × RAG-$1^{-/-}$ host mice in parabionts with diseased IL-$7^{+/+}$ × RAG-$1^{-/-}$ donor mice develop colitis. *A*, Histological examination by H&E staining (*left*) and Alcian blue staining (*right*) of the colon from each group at 4 wk after surgery. Representative of four separate samples in each group. Original magnification, ×100. *B*, Histological scoring of the colon from Groups 1–4 at 4 wk after surgery. Data are indicated as the mean ± SEM of six mice in each group. *, $p < 0.01$, vs Group 1 donors. **, $p < 0.01$, vs Group 1 hosts. Gr., Group.

1 and 4 did not develop colitis. Furthermore, acid mucin production examined by Alcian blue staining revealed a marked decrease of mucin-producing goblet cells in all colitic mice in Groups 2 and 3 in contrast to mice in Groups 1 and 4 (Fig. 2*A*, *right*).

To clarify that newly developed colitis in host mice of Groups 2 and 3 was surely mediated by the infiltration of immigrant $CD4^+$ T cells from donor mice, but not by innate immune cells such as granulocytes and macrophages, we next assessed colonic infiltration of $CD4^+$ T cells by immunohistochemistry. Fig. 3 clearly demonstrated marked infiltration of $CD4^+$ T cells in the colon of host mice as well as in donor mice in parabionts of Groups 2 and 3. In contrast, only a small population of $CD4^+$ T cells was found in the host and donor mice in Groups 1 and 4 (Fig. 3). Especially, although the IL-$7^{+/+}$ × RAG-$1^{-/-}$ host mice in Group 1 had severe wasting disease with symptoms of colitis before surgery, there were only a few infiltrated $CD4^+$ T cells observed in colonic LP, indicating that the previous colitis was suppressed and cured by certain immigrant suppressor cells derived from normal host mice.

We next examined the cytokine production by LP $CD4^+$ T cells from each mouse in Groups 1–4. As shown in Fig. 4, LP $CD4^+$ T cells from donor and host mice in Groups 2 and 3 produced significantly higher amounts of IFN-γ and TNF-α as compared with those from mice in Groups 1 and 4, indicating that colitic LP $CD4^+$ T cells in IL-$7^{-/-}$ × RAG-$1^{-/-}$ host mice or IL-$7^{+/+}$ × RAG-$1^{-/-}$ host mice of Groups 2 and 3 have functions of Th1-mediated immune responses. Importantly, the elevated production of these cytokines in Groups 2 and 3 was dependent on the presence of colitis, but not on the expression of IL-7 in the colon.

Expansion of $CD4^+$ T cells is dependent on IL-7 in the SP or BM but is independent of IL-7 in the LP

We have previously reported that BM retaining colitogenic $CD4^+$ T cells in colitic mice might play a critical role as a reservoir for persisting colitis (18). Furthermore, BM is physiologically a major source of IL-7, contributing to the development of B cells (24). To further investigate the role of intestinal and/or systemic IL-7 in consecutive immunopathology of the parabiosis model, we next compared the composition of $CD4^+$ T cells in the LP, BM, and SP of donor and host mice in each parabiont using flow cytometry at 4 wk after surgery. The recovered cell numbers of $CD3^+CD4^+$ T cells from the donor and host LP in Groups 2 and 3 were significantly higher as compared with those of the paired donor and host colitic mice in Groups 1 and 4 parabionts, respectively (Fig. 5*A*). Furthermore, the recovered cell numbers of $CD3^+CD4^+$ T cells in the donor and host BM (Fig. 5*B*) and SP (Fig. 5*C*) in Groups 2 and 3 were significantly higher as compared with those of the paired donor and host colitic mice in Group 4, but not in Group 1, parabionts, respectively. In contrast, IL-$7^{+/+}$ × RAG-$1^{-/-}$ donor mice that were previously transferred with $CD4^+CD45RB^{high}$ T cells and C57BL/6-Ly5.1 host mice in Group 1 sustained a normal number of cells in the BM and SP (Fig. 5, data not shown). Most importantly, although the number of $CD3^+CD4^+$ T cells recovered from the SP or BM of the IL-$7^{-/-}$ × RAG-$1^{-/-}$ host mice in Group 3 was significantly decreased compared with that of the

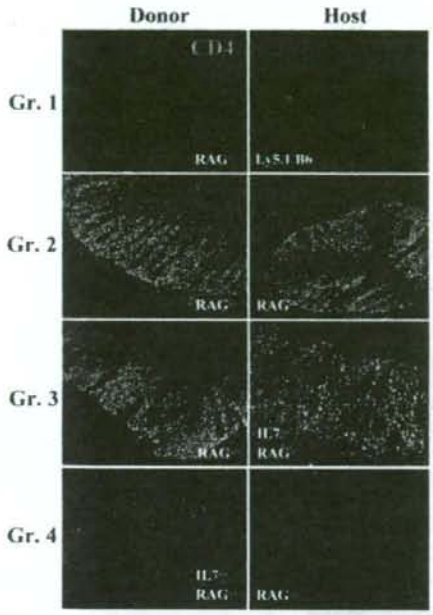

FIGURE 3. IL-7$^{-/-}$ × RAG-1$^{-/-}$ host mice in parabionts developed colitis with the marked infiltration of immigrant CD4$^+$ T cells from donor mice. CD4 immunostaining and DAPI counterstaining of the colon from Groups 1–4 at 4 wk after surgery. Frozen sections were fixed with 4% paraformaldehyde phosphate buffer solution and stained with anti-mouse CD4 mAb, followed by AlexaFluor 488 goat anti-rat IgG as secondary Ab and DAPI counterstaing. A large number of CD4$^+$ T cells were infiltrated in the colonic mucosa of IL-7$^{-/-}$ × RAG-1$^{-/-}$ host mice (Group 3) as well as in that of IL-7$^{+/+}$ × RAG-1$^{-/-}$ host mice (Group 2). Representative of four separate samples in each group. Original magnification: ×100. Gr., Group.

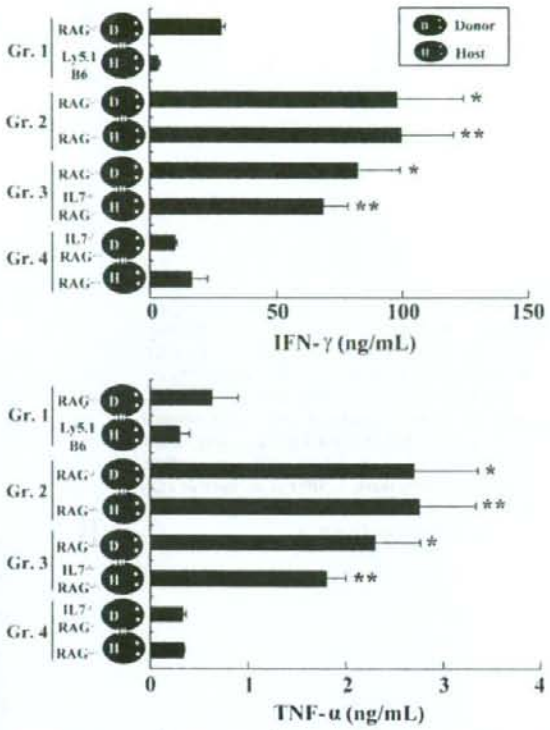

FIGURE 4. IL-7$^{-/-}$ × RAG-1$^{-/-}$ host mice in parabionts develop Th1-mediated colitis. LP CD4$^+$ T cells were prepared from colons at 4 wk after surgery and stimulated with anti-CD3 and anti-CD28 mAbs for 48 h. Concentrations of IFN-γ, and TNF-α in culture supernatants were measured by ELISA. Data are indicated as the mean ± SEM of six mice in each group. *, $p < 0.01$, vs Group 1 donors. **, $p < 0.01$, vs Group 1 hosts. Gr., Group.

IL-7$^{+/+}$ × RAG-1$^{-/-}$ host mice in Group 2, an equivalent number of CD4$^+$ T cells was recovered from the LP of both host mice in Groups 2 and 3, indicating that the expansion of CD4$^+$ T cells in the SP and BM is dependent on IL-7, but is independent in the LP.

Further analysis of Group 1 mice using a four-colored CD3/CD4/Ly5.1/Ly5.2 FACS staining revealed that >95% of total CD4$^+$ T cells were derived from Ly5.1$^+$ cells and most resident Ly5.2$^+$CD4$^+$ T cells decreased to only 5–10% of total CD4$^+$ T cells in SP and BM in Group 1 IL-7$^{+/+}$ × RAG-1$^{-/-}$ donor mice (Fig. 5). Interestingly, although the absolute number of LP CD4$^+$ T cells was significantly decreased in Group 1 IL-7$^{+/+}$ × RAG-1$^{-/-}$ donor mice as compared with those of IL-7$^{+/+}$ × RAG-1$^{-/-}$ donor mice in Groups 2 and 3 colitic parabionts, ~50% of total LP CD4$^+$ T cells remained to be Ly5.2$^+$, suggesting that 1) colitogenic LP Ly5.2$^+$CD3$^+$CD4$^+$ T cells were resistant to the suppression by Ly5.1-derived cells as compared with Ly5.2$^+$CD3$^+$CD4$^+$ T cells in other sites and/or 2) they remained in the intestine, and in other words could not exit, and redistribute outside the intestine. Furthermore, small but substantial percentages (1–5%) of total CD4$^+$ T cells in each tissue of host C57BL/6-Ly5.1 mice were donor-derived Ly5.2$^+$ cells, indicating that two-way recirculation of CD4$^+$ T cells from the donor to the host and vice versa had been established and most of Ly5.2$^+$ colitogenic CD4$^+$ T cells in both donor and host mice had undergone the contraction under a certain suppressive mechanism including suppression by CD4$^+$CD25$^+$Foxp3$^+$ regulatory T cells derived from host C57BL/6 mice.

IL-7 is not detected in host IL-7$^{-/-}$ × RAG-1$^{-/-}$ host mice after parabiosis

Studies showing engraftment of BM-derived cells to various non-hemopoietic tissues including epithelial cells after BM transplantation are now on topic (26, 27), and we have previously demonstrated that human BM cells have a potential to repopulate the gastrointestinal epithelia by detecting Y-chromosomes in female cases that have undergone BM transplantation using male donor cells (28). It was thus needed to assess whether this was the case with our parabiosis setting, and if so, it was interesting to know whether IL-7 was produced by engrafted colonic epithelial cells derived from the BM of IL-7$^{+/+}$ × RAG-1$^{-/-}$ donor mice in IL-7$^{-/-}$ × RAG-1$^{-/-}$ host mice after surgery in Group 3. As shown in Fig. 6*A*, immunohistochemistry revealed that IL-7 is detected in uninflamed colonic epithelia of both IL-7$^{+/+}$ × RAG-1$^{-/-}$ donor and C57BL/6 host mice in Group 1 and IL-7$^{+/+}$ × RAG-1$^{-/-}$ host, but not in IL-7$^{-/-}$ × RAG-1$^{-/-}$ donor, mice in Group 4. Consistent with previous findings (17), IL-7 expression was detectable, but markedly decreased in inflamed colonic epithelia in Groups 2 and 3 of IL-7$^{+/+}$ × RAG-1$^{-/-}$ mice along with the decreased goblet cells, in both host and donor mice (Fig. 2*A*, *right*). In contrast, IL-7 was not detected in the inflamed colonic epithelia of Group 3 IL-7$^{-/-}$ × RAG-1$^{-/-}$ host mice (Fig. 6*A*). Consistent with these results, further RT-PCR analysis for IL-7 mRNA expression showed that IL-7 mRNA was not detected in

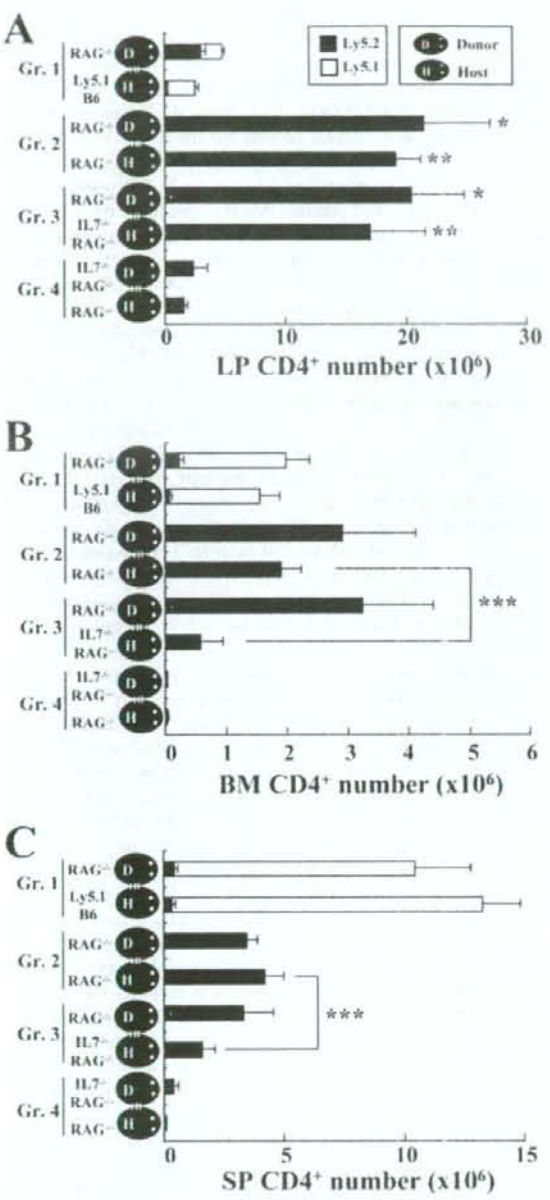

FIGURE 5. Expansion of BM and SP, but not of LP, $CD4^+$ T cells in IL-$7^{-/-}$ × RAG-$1^{-/-}$ host mice in parabionts is dependent on IL-7. LP (*A*), BM (*B*), and SP (*C*) $CD4^+$ T cells were isolated from each mouse of Groups 1–4 at 4 wk after surgery, and the number of $CD4^+$ cells were determined by flow cytometry. Data are indicated as the mean ± SEM of six mice in each group. *, $p < 0.01$, vs Group 1 donors. **, $p < 0.01$, vs Group 1 hosts. ***, $p < 0.01$, vs Group 2 hosts. For cells in Group 1 parabionts, cells were stained with anti-CD45.1 mAb and anti-CD45.2 mAb to discriminate between donor or host origin. Gr., Group.

colitic IL-$7^{-/-}$ × RAG-$1^{-/-}$ host mice in Group 3, and was markedly decreased in colitic IL-$7^{+/+}$ × RAG-$1^{-/-}$ donor and host mice in Groups 2 and 3 in clear contrast to that of control C57BL/6 mice (Fig. 6*B*).

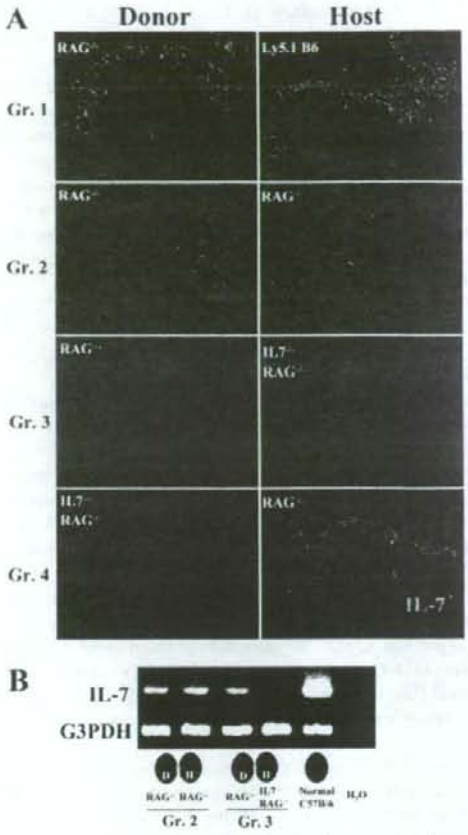

FIGURE 6. IL-7 is not detected in host IL-$7^{-/-}$ × RAG-$1^{-/-}$ mice in parabionts with diseased IL-$7^{+/+}$ × RAG-$1^{-/-}$ donor mice. *A*, Frozen sections of colon from each mouse in Groups 1–4 at 4 wk after surgery were stained with polyclonal anti-IL-7 Abs. Representative of five separate samples in each group. Original magnification: ×100. *B*, Expression of IL-7 mRNA in the whole colon was determined by RT-PCR. Representative of five separate samples in each group. Gr., Group.

Discussion

In this study, we demonstrated that intestinal IL-7 is not essential for the development and perpetuation of colitis by showing that IL-$7^{-/-}$ × RAG-$1^{-/-}$ host mice parabiosed with colitic IL-$7^{+/+}$ × RAG-$1^{-/-}$ donor mice develop a wasting disease and severe colitis. Because we previously demonstrated that IL-7 is needed to develop and sustain colitis by showing a lack of colitis development in IL-$7^{-/-}$ × RAG-$1^{-/-}$ mice transferred with $CD4^+CD45RB^{high}$ T cells or colitogenic LP $CD4^+$ T cells (19), in this study, we suggest that IL-7 production from tissues other than the intestine, such as BM, is sufficient, or rather may be essential to develop and sustain the chronic colitis.

Before starting this study, we confronted a paradox between two facts. The first fact is that IL-7-producing goblet cells are easily decreased or depleted in patients with severe ulcerative colitis (29), colitic IL-7 Tg mice (17) and in the present model of colitis (Fig. 2*A*, *right*) resulting in the decreased IL-7 production in the intestine, and the second fact is that IL-7 appeared to be indispensable for the development and persistence of chronic colitis by adoptive transfer experiment using IL-$7^{-/-}$ × RAG-$1^{-/-}$ mice (19). Based on these backgrounds, we hypothesized that intestinal IL-7 is

indeed important to establish GALT, such as Payer's patches and cryptopatches, and also to maintain IELs (30), but not needed to develop and sustain colitis, since many Ags, such as intestinal bacterial Ags, may be sufficient to stimulate colitogenic $CD4^+$ T cells in the intestinal LP without stimuli from IL-7. To prove it, we performed a combinational experiment using adoptive transfer and parabiosis systems in the present study. Although the parabiosis system seems to be somewhat artificial and problematic on some level as two mice, host and donor, are forced to have a surgical stress and behavioral limitation (Groups 3 and 4), mice laboring colitogenic $CD4^+$ T cells are surgically joined, resulting in prompt development of anastomoses of blood vessels within a few days. Even in the present setting, it is noteworthy that IL-$7^{-/-}$ × RAG-$1^{-/-}$ host mice joined with colitic IL-$7^{+/+}$ × RAG-$1^{-/-}$ donor mice developed a wasting disease and colitis to the similar level of colitic IL-$7^{+/+}$ × RAG-$1^{-/-}$ donor mice over time.

In this parabiosis system, however, it was also possible that certain stem cells that are committed to differentiate into IL-7-producing mesenchymal cells or epithelial cells homed to the intestine, and might have been involved in the development and persistence of colitis in IL-$7^{-/-}$ × RAG-$1^{-/-}$ host mice joined with colitic IL-$7^{+/+}$ × RAG-$1^{-/-}$ donor mice (Group 3). To rule out this possibility, we also demonstrated that IL-7 expression was not detected in the colon of the IL-$7^{-/-}$ × RAG-$1^{-/-}$ host mice both at the protein and mRNA levels (Fig. 6). Consistent with the present result, another group demonstrated that restoring intestinal IL-7 expression to IL-$7^{-/-}$ mice did not result in the development of colitis (31). Collectively, the current results clearly indicate that intestinal IL-7 is not essential, but systemic IL-7 from extraintestinal sites is essential, for the development and sustainment of colitis.

It is also very important to know why IL-7 is decreased in the inflamed mucosa of colitis in terms of pathogenesis of chronic colitis. In other words, it is possible that the lack or decrease of IL-7 production in inflamed mucosa of colitis is pathologically needed to maintain chronic colitis. Consistent with this hypothesis, we previously demonstrated that although IL-7 promoted proliferation of human LP IL-7Rα-expressing $CD4^+$ T cells, double stimuli by IL-7 and anti-CD3 mAb conversely suppressed it (21). In addition, Fluur and colleagues (32) very recently reported that IL-7 induces Fas-mediated T cell apoptosis by inducing Fas expression on $CD4^+$ T cells. Thus, it appears that intestinal IL-7 physiologically plays a key role in the elimination of pathological LP $CD4^+$ T cells activated by intestinal bacteria. Further studies will be needed to address this issue.

Interestingly, the recovered cell number of LP $CD4^+$ T cells was equivalent between host and donor mice both in Group 2 and 3, although it was likely that total production of IL-7 in Group 3 parabionts between one IL-$7^{+/+}$ mouse and one IL-$7^{-/-}$ mouse was approximately half compared with that in Group 2 parabionts between two IL-$7^{+/+}$ mice. Because it seems that the production of IL-7 is maintained at a constant rate and is uninfluenced by extrinsic stimuli (33, 34), this result indicates that factors other than IL-7, such as stimulation by commensal bacteria might control the homeostasis of cell number in the LP, but not in the BM and SP. Further studies will be needed to address this issue.

BM is a major source of IL-7 in the body (26). In contrast to the LP, it is noteworthy that the number of $CD4^+$ T cells recovered from the BM and SP of the colitic IL-$7^{-/-}$ × RAG-$1^{-/-}$ host mice (Group 3) was significantly decreased compared with that of the IL-$7^{+/+}$ × RAG-$1^{-/-}$ host mice. Regarding this result, we recently demonstrated that $CD4^+$ effector-memory-like T (T_{EM}-like) cells reside in the BM of colitic SCID and RAG-$1/2^{-/-}$ mice induced by adoptive transfer of $CD4^+CD45RB^{high}$ T cells (20). Importantly, these resident BM $CD4^+$ T_{EM}-like cells are closely attached to IL-7-producing stromal cells in the colitic BM. Most importantly, the accumulation of BM $CD4^+$ T_{EM}-like cells was significantly decreased in IL-7-deficient recipients reconstituted with the colitogenic LP $CD4^+$ T_{EM}-like cells. Together with the present study, these findings suggest that the BM $CD4^+$ T_{EM}-like cells residing in mice with chronic colitis play a critical role as a reservoir for lifelong persisting colitis in an IL-7-dependent manner. However, it is still possible that IL-7 produced by sites other than intestine or BM, such as skin, liver, eye, lymph nodes (LN), and SP, also contribute to the development and perpetuation of colitis. In this regard, we very recently demonstrated that splenectomized LN-null lymphotoxin $\alpha^{-/-}$ × RAG-$2^{-/-}$ mice transferred with colitogenic LP $CD4^+$ T cells develop colitis (35), suggesting that IL-7 production at least by LN and SP does not appear to be essential. To further clarify the role of IL-7 produced by BM mesenchymal cells in the pathogenesis of chronic colitis, BM chimera of IL-$7^{-/-}$ × RAG-$1^{-/-}$ mice, which are lethally irradiated and transplanted with the BM cells from IL-$7^{+/+}$ × RAG-$1^{-/-}$ mice, may be quite beneficial. Interestingly, however, it is also well known that extraintestinal complications of IBD patients such as skin, liver, and mucocutaneous manifestations (36) appears to be closely associated with sites of local IL-7 production by keratinocytes, hepatocytes, and uvea cells. Although no inflammation was not observed at least in liver and skin in the present model of colitis (data not shown), further studies will be needed to address this issue.

Clinicopathologically, IBD is characterized by chronic intestinal inflammation. Surgery does not cure IBD, especially Crohn's disease, as relapse is a rule after remission, suggesting that IBD is not a circumscribed disease, but rather a systemic disease mediated by colitogenic memory $CD4^+$ T cells distributing throughout the body via the bloodstream, which may hide in their reservoir, such as BM. Consistent with this hypothesis, recent findings showing usefulness of leukocytoapheresis, which removes peripheral blood cells for the treatment of refractory IBD patients (37, 38), suggests that recirculation of colitogenic memory $CD4^+$ T cells from the gut to some reservoir and vice versa, may play a role in the perpetuation of chronic colitis. Furthermore, we have recently demonstrated that FTY720 that has an ability to inhibit circulation of lymphocytes prevents the development of SCID/RAG-$1/2^{-/-}$ colitis induced by adoptive transfer of LP colitogenic $CD4^+$ T_{EM}-like cells (39). Together with the current results, it would be possible that the circulation of colitogenic $CD4^+$ T_{EM}-like cells is quite active in IBD, making them continue to circulate in the blood and migrate to IL-7-producing reservoir from the IL-7-depleted LP.

In summary, in this study, we demonstrated that systemic IL-7, but not intestinal IL-7, is essential for the development and perpetuation of colitis, suggesting that therapeutic approaches targeting systemic IL-7 using the biologics against IL-7 may be feasible in the treatment of IBD.

Acknowledgements

We are grateful to R. Zamoyska for providing mice and K. Suzuki for his technical assistance.

Disclosures

The authors have no financial conflict of interest.

References

1. Podolsky, D. K. 2002. Inflammatory bowel disease. *N. Engl. J. Med.* 347: 417–429.
2. Sands, B. E. 2007. Inflammatory bowel disease: past, present, and future. *J. Gastroenterol.* 42: 16–25.
3. Strober, W., I. J. Fuss, and R. S. Blumberg. 2002. The immunology of mucosal models of inflammation. *Annu. Rev. Immunol.* 20: 495–549.

4. Bamias, G., M. R. Nyce, S. A. De La Rue, and F. Cominelli. 2005. New concepts in the pathophysiology of inflammatory bowel disease. *Ann. Intern. Med.* 143: 895–904.
5. Sartor, R. B. 2006. Mechanisms of disease: pathogenesis of Crohn's disease and ulcerative colitis. *Nat. Clin. Pract. Gastroenterol. Hepatol.* 3: 390–407.
6. Hibi, T., and H. Ogata. 2006. 2006. Novel pathophysiological concepts of inflammatory bowel disease. *J. Gastroenterol.* 41: 10–16.
7. Namen, A. E., S. Lupton, K. Hjerrild, J. Wignall, D. Y. Mochizuki, A. Schmierer, B. Mosley, C. J. March, D. Urdal, and S. Gillis. 1988. Stimulation of B-cell progenitors by cloned murine interleukin-7. *Nature* 333: 571–573.
8. Watanabe, M., Y. Ueno, T. Yajima, Y. Iwao, M. Tsuchiya, H. Ishikawa, S. Aiso, T. Hibi, and H. Ishii. 1995. Interleukin 7 is produced by human intestinal epithelial cells and regulates the proliferation of intestinal mucosal lymphocytes. *J. Clin. Invest.* 95: 2945–2953.
9. Fry, T. J., and C. L. Mackall. 2005. The many faces of IL-7: from lymphopoiesis to peripheral T cell maintenance. *J. Immunol.* 174: 6571–6576.
10. Bradley, L. M., L. Haynes, and S. L. Swain. 2005. IL-7: maintaining T-cell memory and achieving homeostasis. *Trends Immunol.* 26: 172–176.
11. Sprent, J., and C. D. Surh. 2002. T cell memory. *Annu. Rev. Immunol.* 20: 551–579.
12. Jameson, S. C. 2002. Maintaining the norm: T-cell homeostasis. *Nat. Rev. Immunol.* 2: 547–556.
13. Schluns, K. S., and L. Lefrancois. 2003. Cytokine control of memory T-cell development and survival. *Nat. Rev. Immunol.* 3: 269–279.
14. Seder, R. A., and R. Ahmed. 2003. Similarities and differences in $CD4^+$ and $CD8^+$ effector and memory T cell generation. *Nat. Immunol.* 4: 835–842.
15. Ma, A., R. Koka, and P. Burkett. 2006. Diverse functions of IL-2, IL-15, and IL-7 in lymphoid homeostasis. *Annu. Rev. Immunol.* 24: 57–79.
16. Surh, C. D., O. Boyman, J. F. Purton, and J. Sprent. 2006. Homeostasis of memory T cells. *Immunol. Rev.* 211: 154–163.
17. Watanabe, M., Y. Ueno, T. Yajima, S. Okamoto, T. Hayashi, M. Yamazaki, Y. Iwao, H. Ishii, S. Habu, M. Uehira, et al. 1998. Interleukin 7 transgenic mice develop chronic colitis with decreased interleukin 7 protein accumulation in the colonic mucosa. *J. Exp. Med.* 187: 389–402.
18. Yamazaki, M., T. Yajima, M. Tanabe, K. Fukui, E. Okada, R. Okamoto, S. Oshima, T. Nakamura, T. Kanai, M. Uehira, et al. 2003. Mucosal T cells expressing high levels of IL-7 receptor are potential targets for treatment of chronic colitis. *J. Immunol.* 171: 1556–1563.
19. Totsuka, T., T. Kanai, Y. Nemoto, S. Makita, and M. Watanabe. 2007. IL-7 is essential for the development and the persistence of chronic colitis. *J. Immunol.* 178: 4737–4748.
20. Nemoto, Y., T. Kanai, S. Makita, R. Okamoto, T. Totsuka, K. Takeda, and M. Watanabe. 2007. Bone marrow retaining colitogenic $CD4^+$ T cells may be a pathogenic reservoir for chronic colitis. *Gastroenterology* 132: 176–189.
21. Watanabe, M., N. Watanabe, Y. Iwao, H. Ogata, T. Kanai, Y. Ueno, M. Tsuchiya, H. Ishii, S. Aiso, S. Habu, and T. Hibi. 1997. The serum factor from patients with ulcerative colitis that induces T cell proliferation in the mouse thymus is interleukin-7. *J. Clin. Immunol.* 17: 282–292.
22. Powrie, F., M. W. Leach, S. Mauze, L. B. Caddle, and R. L. Coffman. 1993. Phenotypically distinct subsets of $CD4^+$ T cells induce or protect from chronic intestinal inflammation in C. B-17 scid mice. *Int. Immunol.* 5: 1461–1471.
23. Maloy, K., and F. Powrie. 2001. Regulatory T cells in the control of immune pathology. *Nat. Immunol.* 2: 816–822.
24. Seddon, B., P. Tomlinson, and R. Zamoyska. 2003. Interleukin 7 and T cell receptor signals regulate homeostasis of CD4 memory cells. *Nat. Immunol.* 4: 680–686.
25. Totsuka, T., T. Kanai, R. Iiyama, K. Uraushihara, M. Yamazaki, R. Okamoto, T. Hibi, K. Tezuka, M. Azuma, H. Akiba, et al. 2003. Ameliorating effect of anti-ICOS monoclonal antibody in a murine model of chronic colitis. *Gastroenterology* 124: 410–421.
26. Di Rosa, F., and R. Pabst. 2005. The bone marrow: a nest for migratory memory T cells. *Trends Immunol.* 26: 360–366.
27. Korbling, M., and Z. Estrov. 2003. Adult stem cells for tissue repair: a new therapeutic concept? *N. Engl. J. Med.* 349: 570–582.
28. Okamoto, R., T. Yajima, M. Yamazaki, T. Kanai, M. Mukai, S. Okamoto, Y. Ikeda, T. Hibi, J. Inazawa, and M. Watanabe. 2002. Damaged epithelia regenerated by bone marrow-derived cells in the human gastrointestinal tract. *Nat. Med.* 8: 1011–1017.
29. Riddell, R. H. 2004. Pathology of idiopathic inflammatory bowel disease. In *Kirsner's Inflammatory Bowel Diseases*, 6th Ed. R. B. Sartor and W. J. Sandborn, eds. Saunders, Philadelphia, pp. 399–424.
30. Spahn, T. W., and T. Kucharzik. 2004. Modulating the intestinal immune system: the role of lymphotoxin and GALT organs. *Gut* 53: 456–465.
31. Laky, K., L. Lefrancois, E. G. Lingenheld, H. Ishikawa, J. M. Lewis, S. Olson, K. Suzuki, R. E. Tigelaar, and L. Puddington. 2000. Enterocyte expression of interleukin 7 induces development of γδ T cells and Peyer's patches. *J. Exp. Med.* 191: 1569–1580.
32. Fluur, C., A. De Milito, T. J. Fry, N. Vivar, L. Eidsmo, A. Atlas, C. Federici, P. Matarrese, M. Logozzi, E. Rajnavolgyi, et al. 2007. Potential role for IL-7 in Fas-mediated T cell apoptosis during HIV infection. *J. Immunol.* 178: 5340–5350.
33. Mazzucchelli, R., and S. K. Durum. 2007. Interleukin-7 receptor expression: intelligent design. *Nat. Rev. Immunol.* 7: 144–154.
34. Fry, T. J., and C. L. Mackall. 2005. The many faces of IL-7: from lymphopoiesis to peripheral T cell maintenance. *J. Immunol.* 174: 6571–6576.
35. Makita, S., T. Kanai, Y. Nemoto, T. Totsuka, R. Okamoto, K. Tsuchiya, M. Yamamoto, H. Kiyono, and M. Watanabe. 2007. Intestinal lamina propria retaining $CD4^+CD25^+$ regulatory T cells is a suppressive site of intestinal inflammation. *J. Immunol.* 178: 4937–4946.
36. Orchard, T. R., and D. P. Jewell. 2004. Extraintestinal manifestations: skin, joints, and mucocutaneous manifestations. In *Kirsner's Inflammatory Bowel Diseases*, 6th Ed. R. B. Sartor and W. J. Sandborn, eds. Saunders, Philadelphia, pp. 658–872.
37. Kanai, T., T. Hibi, and M. Watanabe. 2006. The logics of leukocytapheresis as a natural biological therapy for inflammatory bowel disease. *Exp. Opin. Biol. Ther.* 6: 453–466.
38. Hibi, T., and A. Sakuraba. 2005. Is there a role for apheresis in gastrointestinal disorders? *Nat. Clin. Pract. Gastroenterol. Hepatol.* 2: 200–201.
39. Fujii, R., T. Kanai, Y. Nemoto, S. Makita, S. Oshima, R. Okamoto, K. Tsuchiya, T. Totsuka, and M. Watanabe. 2006. FTY720 suppresses $CD4^+CD44^{high}$ $CD62L^-$ effector memory T cell-mediated colitis. *Am. J. Physiol.* 291: G267–G274.

Bone Marrow Retaining Colitogenic CD4+ T Cells May Be a Pathogenic Reservoir for Chronic Colitis

YASUHIRO NEMOTO,* TAKANORI KANAI,* SHIN MAKITA,* RYUICHI OKAMOTO,* TERUJI TOTSUKA,* KIYOSHI TAKEDA,‡ and MAMORU WATANABE*

*Department of Gastroenterology and Hepatology, Graduate School, Tokyo Medical and Dental University, Tokyo, Japan; and ‡Department of Molecular Genetics, Medical Institute for Bioregulation, Kyushu University, Fukuoka, Japan

Background & Aims: **Although bone marrow (BM) is known as a primary lymphoid organ, it also is known to harbor memory T cells, suggesting that this compartment is a preferential site for migration and/or selective retention of memory T cells. We here report the existence and the potential ability to induce colitis of the colitogenic BM CD4+ memory T cells in murine colitis models.** ***Methods:*** **We isolated BM CD4+ T cells obtained from colitic severe combined immunodeficient mice induced by the adoptive transfer of $CD4^+CD45RB^{high}$ T cells and colitic interleukin (IL)-$10^{-/-}$ mice that develop colitis spontaneously, and analyzed the surface phenotype, cytokine production, and potential activity to induce colitis. Furthermore, we assessed the role of IL-7 to maintain the colitogenic BM CD4+ T cells.** ***Results:*** **A high number of CD4+ T cells reside in the BM of colitic severe combined immunodeficient mice and diseased IL-$10^{-/-}$ mice, and they retain significant potential to induce type-1 T helper-mediated colitis in an IL-7–dependent manner. These resident BM CD4+ T cells have an effector memory (T_{EM}; $CD44^{high}CD62L^{-}IL\text{-}7R^{high}$) phenotype and preferentially are attached to IL-7–producing BM cells. Furthermore, the accumulation of BM CD4+ T_{EM} cells was decreased significantly in IL-7–deficient recipients reconstituted with the colitogenic lamina propria CD4+ T_{EM} cells.** ***Conclusions:*** **Collectively, these findings suggest that BM-retaining colitogenic CD4+ memory T cells in colitic mice play a critical role as a reservoir for persisting lifelong colitis.**

BASIC—ALIMENTARY TRACT

It has long been known that T-cell precursors generated in the bone marrow (BM) migrate to the thymus, where T-cell development occurs. However, a fact often neglected is that under physiologic conditions, mature CD4+ and CD8+ T cells undergo extensive migration from the blood to the BM and vice versa. In both human beings and mice, T-cell receptor $\alpha\beta^+$ cells constitute approximately 3%–8% of nucleated BM cells.[1,2] BM CD4+ and CD8+ T-cell populations contain a high proportion of cells displaying a memory phenotype, that is, expressing low levels of CD45RA in human beings[3] and high levels of CD44 in mice.[4,5]

As early as 1974 it was documented that mouse CD4+ T cells migrate to the BM after priming, and it was proposed that BM CD4+ T cells contributed to the development of a memory antibody response in this organ.[6] Recently, T cells persisting in extralymphoid organs such as the liver, lung, and skin have attracted increasing interest because it has been recognized that these T cells contribute considerably to the long-lived memory T-cell pool.[7,8] In this context, BM has been shown to harbor a high number of antigen-specific CD8+ T cells for several months after resolution of acute infection.[9] For instance, adoptive transfer of BM cells from lymphochoriomeningitis virus–immune mice (>90 days after acute infection) to immunodeficient recipients provides antiviral protection, and thus CD8+ memory T cells from the BM are able to mount an effective secondary response.[10]

Primary T-cell responses to blood-borne antigens also can be initiated in the BM. This was shown initially in conditions of altered lymphocyte trafficking in splenectomized mice and then in individuals with normal lymphoid organs, for both CD4+ and CD8+ T-cell responses.[11] Thus, the BM resembles a secondary lymphoid organ, although it lacks the organized T- and B-cell areas found in the spleen, lymph nodes, and Peyer's patches. Although accumulating evidence suggests that BM plays an important role in the communication with mature naive/memory T cells, there is no evidence for the role of BM memory CD4+ cells in chronic immune diseases, such as inflammatory bowel diseases (ulcerative colitis and Crohn's disease) and autoimmune diseases. Crohn's disease is characterized by chronic inflammation of the small and large intestine and structures apart from the

Abbreviations used in this paper: Ag, antigen; APC, antigen-presenting cell; BM, bone marrow; BrdU, bromodeoxyuridine; CBA, cecal bacterial antigen; CSFE, carboxyfluoroscein succinimidyl ester; ELISA, enzyme-linked immunosorbent assay; FITC, fluorescein isothiocyanate; IFN, interferon; IL, interleukin; LP, lamina propria; mAb, monoclonal antibody; MLN, mesenteric lymph node; PE, phycoerythrin; SCID, severe combined immunodeficient; Th1, type-1 T helper.

0016-5085/07/$32.00
doi:10.1053/j.gastro.2006.10.035

bowel. Surgery does not cure Crohn's disease, and recurrence after surgery is the rule rather than the exception.[12] There is also no correlation between recurrence of the disease and the dissection of regional lymph nodes and spleen.[13] The evidence suggests that other sites might play a critical role in the recurrence of diseases as reservoirs of colitogenic memory $CD4^+$ T cells.

Furthermore, it is well known that interleukin (IL)-7 is important as a critical factor for the survival and homeostatic proliferation of memory $CD4^+$ T cells, and that BM is a major site of IL-7 production.[14] We have shown previously that mucosal $CD4^+$ T cells in colitic mice express IL-7Rα highly, and they are pathogenic cells responsible for chronic colitis.[15] In vitro stimulation of these colitic lamina propria (LP) $CD4^+IL\text{-}7R^{high}$ T cells by IL-7, but not IL-15 and thymic stromal lymphopoietin, enhanced significant proliferative responses and survival of colitic $CD4^+$ T cells.[16] These backgrounds prompted us to investigate the role of the resident BM memory $CD4^+$ T cells in persisting lifelong colitis using a murine model of chronic colitis induced by the adoptive transfer of $CD4^+CD45RB^{high}$ T cells.

Materials and Methods

Mice

Female BALB/c, CB-17 severe combined immunodeficient (SCID), and C57BL/6 mice were purchased from Japan Clea (Tokyo, Japan). Female C57BL/6 Rag-$2^{-/-}$ mice were provided by Central Laboratories for Experimental Animals (Kawasaki, Japan). C57BL/6 Rag-$1^{-/-}$ mice and IL-$7^{-/-}$ mice were kindly provided by Dr. Zamoyska (National Institute for Medical Research, London, UK).[17] IL-$7^{-/-}$ × Rag-$1^{-/-}$ mice and littermate IL-$7^{+/+}$ × Rag-$1^{-/-}$ mice were generated in our laboratory. All mice were maintained under specific-pathogen-free conditions in the Animal Care Facility of the Tokyo Medical and Dental University. The Institutional Committee on Animal Research approved the experiments.

Antibodies and Flow Cytometry

The following monoclonal antibodies (mAbs) other than biotin-conjugated anti-mouse IL-7Rα (A7R34; Immuno-Biological Laboratories, Takasaki, Japan) were obtained from BD PharMingen (San Diego, CA) and used for purification of cell populations and flow-cytometric analysis: Fcγ (CD16/CD32)-blocking mAb (2.4G2), phycoerythrin (PE)-, peridinin chlorophyll protein, and phycoerythrin-phycoerythrin- 5'- disulfonatoindodicarbocyanine conjugated anti-mouse CD4 (RM4-5); fluorescein isothiocyanate (FITC)-conjugated anti-mouse CD3 (145-2C11); PE- and allophycocyanin-conjugated anti-mouse CD44 (IM7); FITC- and PE-conjugated anti-mouse CD62L (MEL-14); FITC-conjugated anti-mouse CD69 (H1.2F3); PE-conjugated anti-mouse integrin $\alpha_4\beta_7$ (DATK32); FITC-conjugated anti-mouse CD45RB (16A); FITC-conjugated hamster anti-mouse Bcl-2 (3F11); PE-conjugated streptavidin; biotin-conjugated rat IgG2; PE-conjugated mouse IgG; and PE-conjugated rat IgG. Flow cytometric 3-color analysis was performed as described.[18]

Induction of Colitis

Colitis was induced in SCID/Rag-$2^{-/-}$ mice by the adoptive transfer of $CD4^+CD45RB^{high}$ T cells as described.[18] Colitic mice were killed at 6–8 weeks after transfer, and $CD4^+$ T cells were isolated from BM, mesenteric lymph nodes (MLNs), and colonic LP.

Cytokine Enzyme-Linked Immunosorbent Assay

To measure cytokine production, 3×10^4 $CD4^+$ T cells from MLN, LP, and BM were cultured in 200 μL of culture medium at 37°C in a humidified atmosphere containing 5% CO_2 in 96-well plates (Costar, Cambridge, MA) precoated with 5 μg/mL hamster anti-mouse CD3ε mAb (145-2C11; BD PharMingen) and 2 μg/mL hamster anti-mouse CD28 mAb (37.51; BD PharMingen) in phosphate-buffered saline (PBS) overnight at 4°C. Culture supernatants were removed after 48 hours and assayed for cytokine production. Cytokine concentrations were determined by specific enzyme-linked immunosorbent assay (ELISA) as per the manufacturer's recommendation (R&D, Minneapolis, MN).

Interferon-γ Production by $CD4^+$ T Cells Stimulated With APCs Pulsed With Cecal Extracts

Colitic SCID mice were killed and their cecums were removed. The cecums were opened and placed in 1 mL of PBS, and the cecal bacteria were expelled by mixing with a vortex, and residual cecal tissue was removed. After the addition of DNase (10 μg/mL), 1 mL of this bacterial suspension was added to 1 mL of glass beads.[19] The cells were disrupted at 5000 revolutions per minute in a Mini-Bead Beater (BioSpec Products, Bartlesville, OK) for 3 minutes and then iced. The glass beads and unlysed cells were removed by centrifuging at 5000 × g for 5 minutes. The lysates were filter-processed in a similar manner. For antigen-presenting cells (APCs), spleen cells from normal BALB/c mice were prepared and treated with the appropriate concentration of cecal bacterial antigens (CBAs) as indicated at 2×10^7 cells/5 mL in a 15-mL tube overnight at 37°C. After washing twice, these APCs were treated with mitomycin-c before being added to T-cell cultures. BM, MLN, and LP $CD4^+$ T cells obtained from normal mice and colitic $CD4^+CD45RB^{high}$ T-cell–transferred SCID mice were cultured in the presence of APCs pretreated with cecal extract antigens in complete media. The culture supernatants were collected on day 3 of culture for interferon (IFN)-γ assay by ELISA.